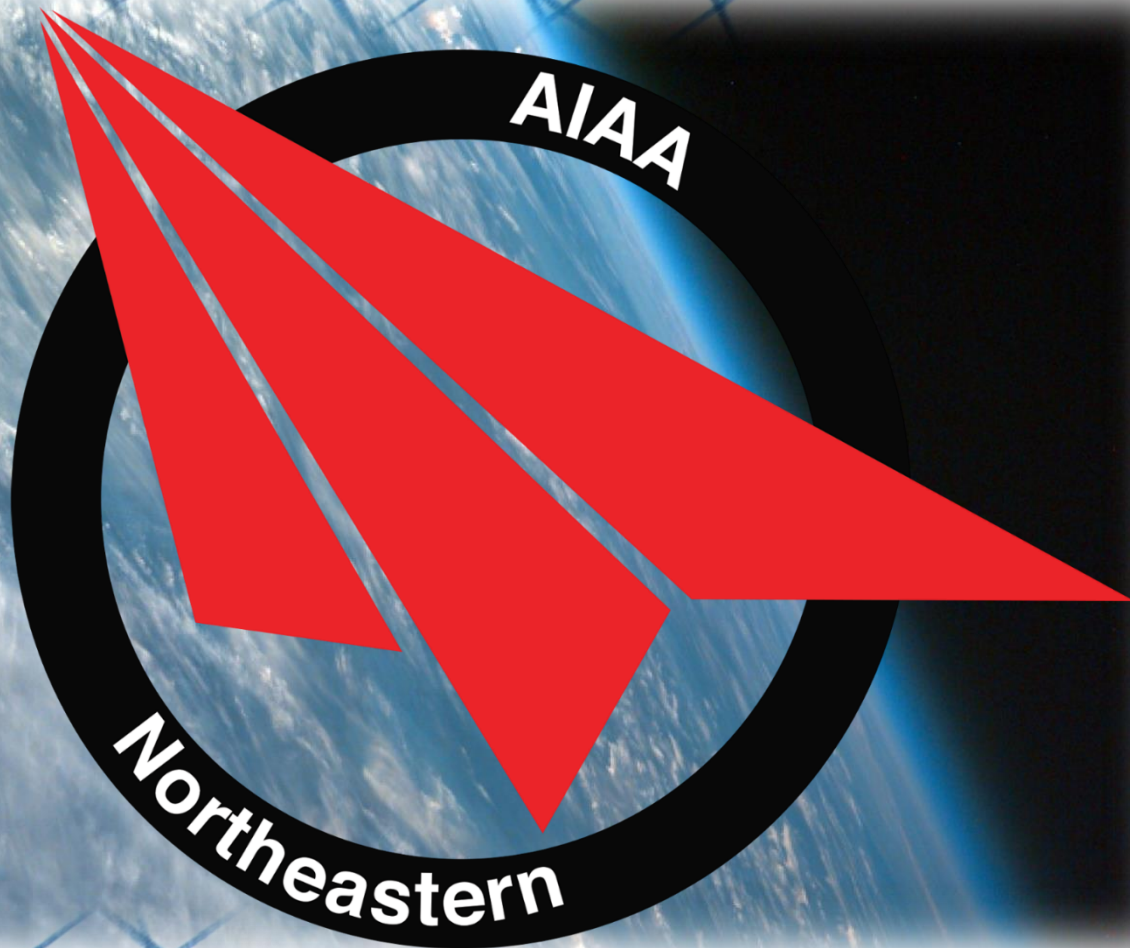




NUSPACE

**Scientific Payloads: Atmospheric-Measurement
and Controlled-Descent Experiment**



**Northeastern University
267 Snell Engineering
Boston, MA 02115**

**2015-2016
NASA Student Launch
Preliminary Design Review**

TABLE OF CONTENTS

| | |
|--|----------|
| 1. SUMMARY | 4 |
| 2. CHANGES MADE SINCE PROPOSAL | 5 |
| 3. VEHICLE CRITERIA | 6 |
| 3.1. Selection, Design, and Verification | 6 |
| 3.1.1. Mission Statement | 6 |
| 3.1.2. System Review | 7 |
| 3.1.3. Subsystem Descriptions..... | 8 |
| 3.1.4. Performance Characteristics | 8 |
| 3.1.5. Verification Plans | 9 |
| 3.1.6. Project Risk Assessment | 10 |
| 3.1.7. Understanding of Components..... | 10 |
| 3.1.8. Manufacturing and Testing..... | 11 |
| 3.1.9. Maturity of Design..... | 11 |
| 3.1.10. Dimensional Drawing | 12 |
| 3.1.11. Electrical Schematics..... | 12 |
| 3.1.12. Mass Statement..... | 13 |
| 3.2. Recovery System | 14 |
| 3.2.1. Analysis | 14 |
| 3.2.2. Major Components..... | 15 |
| 3.3. Mission Performance Prediction | 15 |
| 3.3.1. Mission Performance Criteria..... | 15 |
| 3.3.2. Flight Simulations..... | 16 |
| 3.3.3. Stability Margin | 16 |
| 3.3.4. Kinetic Energy..... | 17 |
| 3.3.5. Drift..... | 18 |
| 3.4. Interfaces and Integration..... | 18 |
| 3.4.1. Payload Integration Plan | 18 |
| 3.4.2. Internal Interfaces | 19 |
| 3.4.3. Vehicle and Ground Interfaces..... | 19 |
| 3.4.4. Vehicle and Ground Launch System Interfaces | 20 |
| 3.5. Safety..... | 20 |
| 3.5.1. Preliminary Checklist | 20 |

| | |
|--|-----------|
| 3.5.2. Safety Officer | 22 |
| 3.5.3. Preliminary Hazard Analysis | 22 |
| 3.5.4. Environmental Concerns..... | 23 |
| 4. PAYLOAD CRITERIA..... | 24 |
| 4.1. Selection, Design, and Verification - CDLE..... | 24 |
| 4.1.1. System Review | 24 |
| 4.1.2. Subsystem Descriptions..... | 29 |
| 4.1.3. Performance Characteristics | 30 |
| 4.1.4. Verification Plan..... | 35 |
| 4.1.5. Preliminary Integration Plan | 37 |
| 4.1.6. Precision and Repeatability..... | 40 |
| 4.1.7. Drawings and Electrical Schematics | 41 |
| 4.1.8. Key Components | 42 |
| 4.2. Concept Features and Design - CDLE | 45 |
| 4.2.1. Creativity and Originality | 45 |
| 4.2.2. Uniqueness and Significance..... | 45 |
| 4.2.3. Challenge Assessment | 46 |
| 4.3. Science Value - CDLE | 46 |
| 4.3.1. Objectives | 46 |
| 4.3.2. Success Criteria..... | 46 |
| 4.3.3. Logic and Approach | 46 |
| 4.3.4. Testing and Variables | 47 |
| 4.3.5. Relevance of Data | 47 |
| 4.3.6. Preliminary Experiment Process | 48 |
| 4.4. Selection, Design, and Verification - ATMOS | 49 |
| 4.4.1. System Review | 49 |
| 4.4.2. Subsystem Descriptions..... | 49 |
| 4.4.3. Performance Characteristics | 50 |
| 4.4.4. Verification Plan..... | 50 |
| 4.4.5. Preliminary Integration Plan | 52 |
| 4.4.6. Precision and Repeatability..... | 52 |
| 4.4.7. Drawings and Electrical Schematics | 54 |
| 4.4.8. Key Components | 55 |
| 4.5. Concept Features and Design - ATMOS | 55 |
| 4.5.1. Creativity and Originality | 55 |

| | |
|---|-----------|
| 4.5.2. Uniqueness and Significance | 56 |
| 4.5.3. Challenge Assessment | 56 |
| 4.6. Science Value - ATMOS | 57 |
| 4.6.1. Objectives | 57 |
| 4.6.2. Success Criteria..... | 57 |
| 4.6.3. Experimental Approach and Rationale | 58 |
| 4.6.3.1. Analog Sensors | 58 |
| 4.6.3.2. Visible Imaging..... | 59 |
| 4.6.3.3. NDVI | 59 |
| 4.6.3.4. Atmospheric Transmittance and Thermal Imaging..... | 59 |
| 4.6.4. Preliminary Experiment Process | 60 |
| 4.6.4.1. Analog Sensors | 61 |
| 4.6.4.2. Visible Imaging | 61 |
| 4.6.4.3. NDVI | 61 |
| 4.6.4.4. Atmospheric Transmittance and Thermal Imaging..... | 61 |
| 5. PROJECT PLAN | 61 |
| 5.1. Budget Plan | 61 |
| 5.2. Funding Plan | 65 |
| 5.3. Timeline | 65 |
| 5.4. Educational Engagement | 66 |
| 5.4.1. Goal of Education and Outreach | 66 |
| 5.4.2. Schedule of Coming Events..... | 67 |
| 5.4.3. Description of Coming Events | 67 |
| 5.4.4. Overall Status | 69 |
| 6. CONCLUSION | 69 |
| APPENDIX A: Milestone Flysheet | 71 |

1. SUMMARY

Northeastern University AIAA

267 Snell Engineering
Northeastern University
Boston, MA 02115

Mentor

Robert DeHate
President AMW/ProX
NAR L3CC 75198 TRA TAP 9956
robert@amwprox.com
(978) 766-9271

The launch vehicle, to be named at a later date, has a total length of 127 inches (approximately 10.5ft) and a diameter of 7.5 inches. The mass of the launch vehicle without the motor is 39.64lb (17.98kg). Given the size and mass of the rocket, we selected the Cesaroni L1115 as the best motor for the competition. The L1115 has an average thrust of 1119 N and a burn time of 4.5s. This motor has a mass of 9.71lb (4.40 kg), bringing the mass of the launch vehicle on the launch pad to a total of 49.35lb (22.38kg). The recovery system for our launch vehicle is unique due to the nature of one of our payloads, which functions both as a payload and a recovery component. The Controlled Descent and Landing Experiment (CDLE) acts as both an engineering payload and the recovery system for the other payload: the Atmospheric and Topographic Measurement Optics Suite (ATMOS). The CDLE will deploy shortly after apogee and descend to a predetermined GPS location. The CDLE deploys from the center of the launch vehicle, leaving the nose cone section, payload section, and motor section to descend using conventional methods. The nose cone section will deploy an 18 inch drogue parachute at apogee. Around the same time, the motor section, still attached to the payload section, will deploy two 18 inch drogue chutes. At 650ft, a 48 inch main parachute will deploy between the previously attached payload and motor sections. For more information regarding the launch vehicle, see the Milestone Review Flysheet Summary located in Appendix A.

One of the two payloads contained in the launch vehicle is the Controlled Descent and Landing Experiment, henceforth denoted as CDLE. This experiment explores the possibility of fully controlled descent and landing, an idea that Northeastern's chapter of the AIAA has been intrigued with since our founding three years ago. The CDLE, for the purposes of the Student Launch competition, is a custom collapsible quadcopter capable of being stored within a 7.5 inch diameter launch vehicle and deployed at high altitudes. The CDLE will be programmed to land at a specified GPS location within the boundaries of Bragg Farms in Toney, Alabama. The CDLE is particularly useful for this competition, as it ensures the safe return and stable orientation of our second payload- ATMOS.

The Atmospheric and Topographic Measurement Optics Suite, henceforth referred to as ATMOS, is the second payload contained within the launch vehicle. ATMOS fulfills the requirements of the atmospheric measurement payload proposed by NASA, measuring humidity, pressure, temperature, solar irradiance, and ultraviolet radiation. In addition, a near infrared spectrum camera will analyze the vegetation present in the field of view and a long-wave infrared spectrum camera will conduct thermal imaging of the surface. The data obtained will be used to calculate the absorption coefficient of the low atmosphere.

2. CHANGE MADE SINCE PROPOSAL

The proposed launch vehicle was divided into four sections: the booster section, the recovery section, the Payload Containment Module (PCM), and the payload deployment section. Those four sections have evolved into three new sections: the nose cone section, a motor section, and the payload section. This is the terminology we will use to refer to the sections while the rocket is assembled. After apogee, the rocket will split into four descending sections, consisting of the three intact launch vehicle sections plus the CDLE. The proposed motor section originally housed a 75mm motor mount tube and three centering rings to ensure the motor stays aligned throughout launch operations. The proposed recovery section was composed of three subsections. There was a 10 inch long interconnector section between the motor section and the electronics bay and recovery section. This is no longer a part of the design. The 75mm motor mount tube and three centering rings are still relevant, however the motor section is now connected to the payload section during descent until 650ft. At 650ft, a 48 inch main parachute will deploy between the two sections, to be attached via shock cord. Two 18 inch drogue parachutes are integrated into the motor section to stabilize the payload section for the release of the CDLE. These are deployed shortly after apogee. The center rings in the motor section will keep the PVC pipes that hold the parachutes aligned within the motor section. The proposed payload containment module has evolved into a more sophisticated and reliable design. This revised design involves a mechanical lock release system for the CDLE. This section, the payload section, is 44 inches long to accommodate the CDLE and the mechanics releasing it. In the proposal, the recovery system relied on a black powder charge that would separate the nose cone and the PCM, releasing an 18 inch upper parachute. A second 18 inch parachute and a 48 inch main parachute would be deployed above the booster section using a Tender Descender. This has been changed to reflect the new configuration. Instead, a single 18 inch parachute will deploy from the nose cone section at apogee.

Since the proposal, we have made numerous changes, including changes to the deployment method, integration into the launch vehicle, and various systems within the CDLE.

Within the CDLE, we changed the method that unfolds the arms. Originally, we had a spring push a bearing up, pivoting the arms downward until a locking mechanism secured them in place. We changed this however, to a lead screw and a matching bearing that is placed in the center of the arms. As the lead screw turns, the bearing moves upward, pivoting the arms down until they are secured in place using a similar locking mechanism.

We also changed the carbon fiber tubes that constitute the arms. Instead of the $\frac{3}{4}$ inch OD carbon fiber tubes, we opted for a larger 1 inch by 1 inch square carbon fiber tubing because it is more resilient to bending. In the proposal, a propeller size was never set, but we opted for a 15 $\frac{1}{2}$ inch propeller, because it provided enough thrust to lift the quadcopter, while being small enough to minimize weight and fit inside the launch vehicle. The largest differences however exist in the deployment method and therefore the launch vehicle integration. The original deployment method of the CDLE was a dual-deployment system, which utilized a drogue deployed at apogee to break shear pins holding the CDLE in place. In the new design, a spring inside the launch vehicle is pushed against the bottom of electronic console that will push the CDLE out of the sheath when the metal clamps are disengaged. Also, originally, the CDLE was oriented so that the propellers were nearest to the nose cone, however in the new design, this orientation was flipped to add the weight of the electronics console nearer to the nose cone.

While the design for the ATMOS has remained relatively constant, the objective has incurred a couple notable changes. Since AIAA at NEU proposed the design for the ATMOS payload, the number of experimental measurements that will be obtained has been reduced from seven to six. The measurements that will be obtained are the following: temperature, pressure, relative humidity, solar irradiance, UV radiation, atmospheric transmittance, and NDVR derived plant density. The measurement that has been eliminated was an original idea that would have calculated albedo, the fraction of the solar energy that Earth reflects back to space. While this would be an intriguing measurement to look into, the ATMOS will focus resources more heavily on the required measurements and the two additional measurements. An additional change will be the altitude that the quadcopter will hover at. It was proposed that the quadcopter would hover 5,280 feet above the ground. Due mostly to the constraints on the CDLE battery life, the quadcopter will undergo controlled descent after deployment and then hover at a lower altitude to obtain the necessary images. Lastly, instead of using a photovoltaic panel to measure solar irradiance, the ATMOS will feature a single photodiode. This will be a more reliable system and will enable more accurate measurements.

There have been few changes to the project plan since the proposal was submitted. The funding plan is heavy on corporate sponsorships, however we are still in the university approval phase of that process. As a result, there has been limited progress with external funding. No changes were made to the internal funding plan; for more information on the progress of internal funding see Section 5.2. The budget plan has seen very few changes as well. While the design has evolved since the proposal, the cost and quantity of the materials have remained nearly constant. The educational engagement plan has hit a few minor speed bumps due to the need for suitable weather conditions. The activity that AIAA runs for the STEM department during middle school field trips (“Paper Rockets”) involves going outside to a common area on campus and using a bike pump to launch students’ paper rocket creations. One of our scheduled field trips was cancelled due to rain, so in order to reach our 200 student goal by the end of the semester we will be looking to add additional STEM events to our schedule.

3. VEHICLE CRITERIA

3.1 Selection, Design, and Verification

3.1.1 Mission Statement

The objectives of Northeastern University’s Student Chapter of the American Institute of Aeronautics and Astronautics are to (1) design, build, launch, and recover a high-powered sounding launch vehicle to an altitude of 5,280 ft. above ground level, and (2) deploy the CDLE containing the ATMOS that will perform atmospheric measurements during descent, including pressure, temperature, relative humidity, solar irradiance, UV radiation, vegetation density, atmospheric transmittance and surface topography and (3) safely land the CDLE and all of the launch vehicle pieces.

Success will be achieved once the ATMOS has collected all of the atmospheric measurements and taken five successful photos in the correct orientation during the descent. In addition, the CDLE will land in a designated safe location to protect valuable information for further analysis upon landing and to prevent injury. Finally, all pieces of the launch vehicle will land within the designated launch field at a safe velocity.

3.1.2 System Review

The launch vehicle's thrust system is composed of a composite motor: the L1115 motor. The specifications of this motor are listed in Table 3.1.2 below.

Table 3.1.2.1 – L1115 specifications

| | |
|----------------|-----------------------|
| Manufacturer | Cesaroni Technologies |
| Name | L1115 |
| Diameter | 75mm |
| Average Thrust | 1119.0N |
| Maximum Thrust | 1713.3N |
| Total Impulse | 5015.0Ns |
| Burn Time | 4.5s |

The motor will be secured in place by a 75.9 mm motor tube and will be centered using 188.1 mm OD and 75.9 mm ID centering rings. The bulkheads will be placed at structurally critical points throughout the rocket to protect important subsystems from ejection charges, including the electronics bays, parachutes, and quadcopter. These structural components will be secured using heat resistant epoxy. Finally, the body of the launch vehicle is designed to separate into 4 sections. The 4 sections are the nose cone, the CDLE, the payload, and the motor. The nose cone section will separate from the rest of the rocket and deploy an 18 inch drogue chute at apogee. The motor section of the rocket will deploy two drogue chutes using blast caps from two PVC tubes that are both equidistant and parallel to the empty motor casing. The CDLE will be released from the motor section and out of the payload section using a release mechanism. The payload section is designed to separate from the motor section using an ejection charge at 650 feet above the ground during descent. A main parachute of diameter 48 inches is deployed from between the payload and the motor sections which are tethered together with shock cord.

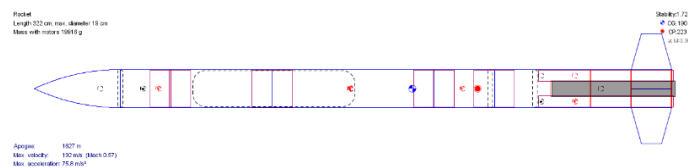


Figure 3.1.2.2 – Launch vehicle layout

This design was chosen because it meets all mission criteria while staying as simple as possible. Another design that was considered included a piston which deployed CDLE by breaking shear pins at apogee. This was determined to be too complicated to be reliable. The current design employs gravity to ensure that the CDLE is deployed in a predictable way every time.

The controlled descent of the nosecone, payload and motor sections has gone under several iterations. Previously, a main would be deployed from the nose cone section and the motor section would deploy two main parachutes from the bottom of the rocket. This configuration was ultimately abandoned due to excessive drifts. The current configuration achieves a reasonable lateral drift distance (less than a mile for all sections) and acceptable kinetic energies at landing for all independent sections.

3.1.3 Subsystem Descriptions

The launch vehicle separates into 4 main sections. The four sections include: (1) the motor section, (2) the payload section, (3) the CDLE, and (4) the nose cone section. The nose cone section will deploy at apogee via an ejection charge controlled by an electronic bay located near the nose cone. An 18 inch drogue will deploy from the nose cone, and this independent section will fall to the ground in accordance with the kinetic energy parameters. Once this is deployed, the two (2) 18 inch drogues will deploy from the two parallel PVC tubes from the motor tube of the launch vehicle. The inner ends of the PVC tubes are connected to blast caps with black powder armed inside. These, too, are controlled by an electronic bay that will provide an ejection charge to release both drogues at apogee. The size of the two drogues allow for proper orientation (motor section facing upwards), establishing a stable platform to release CDLE. Furthermore, the size allow for a smaller drift distance. Upon deployment of the two drogues, there will be a five second delay, allowing for CDLE to be in a proper orientation before the releasing mechanism occurs. The payload section will then begin its separation mechanism, releasing CDLE. The release mechanism consists of a base above the quadcopter. Attached to this base are arms which latch to CDLE. A threaded rod running through the base of the mechanism is rotated by an electric motor which will cause the arms to unlatch from CDLE and release it. Once CDLE is released, it will begin its autonomous controlled descent. At 650ft the payload section will separate from the motor section, remaining tethered to the motor section, and deploy a 48 inch main parachute to achieve kinetic energy and drift parameters until it reaches the ground.

3.1.4 Performance Characteristics

Several key characteristics of the launch vehicle were taken into account to ensure a successful launch. To successfully launch to one mile and deploy scientific payloads, aspects such as the material, releasing mechanism, and electronic components were selected. Vital material decisions were determined based upon material properties, such as durability. The body and coupler tubes of the rocket will be constructed out of blue tube, since it is a durable material that will support the large motor and vehicle body. Furthermore, the fins of the launch vehicle will be made of fiberglass, a reinforced rigid plastic.

The material and construction of the launch vehicle and be evaluated after a launch by visually inspecting the integrity of the vehicle. The releasing mechanism, located in the payload section of the launch vehicle, was another vital characteristic to the rocket's performance. The mechanical lock must be able to react quickly to separate the CDLE from the payload section using mechanical locks and ejection charges. This mechanism will be evaluated by its success of deploying the quadcopter in a reliable way. This can be tested on the ground to some extent, but we will need to test this on a full scale to evaluate this characteristic. In addition, the separations from each section must be accomplished using the

ejection charges at the appropriate times. This allows the CDLE to deploy at more stable conditions, since the drogue parachutes in the back of the motor section allow for a five second orientation/stabilization buffer. The separations will be tested on the ground and in the subscale launch to ensure that they will occur without causing any issues with other aspects of the mission.

3.1.5 Verification Plans

Table 3.1.5 – Launch vehicle verification plan

| Requirement | Plan to Address | Verification Procedure |
|--|---|---|
| The launch vehicle must reach an altitude of one mile above ground level | The launch vehicle will be powered by a L115 rocket motor, which according to simulations on Open Rocket, will take the launch vehicle to an altitude one mile. | A subscale of the final rocket will be built to test the launch vehicle’s ability to reach an altitude of one mile. Once the full scale is built, the full scale will be launched several times to ensure the launch vehicle can reach an altitude of one mile, which will be confirmed by an altimeter. |
| The launch vehicle shall be reusable and relaunchable | The launch vehicle will be constructed out of highly durable materials such as blue tube and PVC to mitigate risk of damage. | Both the subscale and the full scale launch vehicles will be launched several times in order to ensure that the launch vehicle is reusable and relaunchable. Post-launch, the launch vehicle will be thoroughly inspected by the launch vehicle team in order to record any damage incurred during launch and recovery. |
| The launch vehicle will be capable of sitting on the launch pad for one hour with full functionality of all launch components. | All electronics within the rocket will be internally powered and will have enough spare power in order to ensure function for at least one hour. | Post launch, the team will inspect each section to ensure that all systems functioned properly. |
| The launch vehicle shall be capable of being prepared for launch within two hours. | All circuitry on the rocket shall be controlled by switches, in order to ensure simple activation procedures. The CDLE will have a guiding mechanism to ensure ease of insertion in the rocket. | The launch vehicle team will practice and time pre-flight preparation of the launch vehicle before the competition. |

3.1.6 Project Risk Assessment

Table 3.1.6 – Launch vehicle risk assessment

| Risk | Effect | Proposed Mitigations | Likelihood | Impact |
|---|--|---|------------|-------------|
| Missed launch dates, slow construction and/or testing | Miss deadlines, have no working launch vehicle on launch day. | Construct and test on a schedule allowing for mistakes and slow downs. | Medium | Low-High |
| Running out of resources | Inability to construct launch vehicle as designed (leading to undesirable changes in other components of project and increasing the likelihood of running out of funds). | Ensure all necessary parts and equipment are available to use or purchase. | Low | Medium |
| Running out of money in the budget | Inability to afford launch vehicle as designed (leading to cuts in other components of project). | Check prices of all necessary parts and equipment to insure total price does not exceed budget. | Medium | Medium |
| Functionality | Inability to reach target altitude, deploy quadcopter properly, or descend in a controlled and safe manner. | Devote large amounts of time and effort to constructing and testing all components of the launch vehicle. Schedule time for redesigning and rebuilding in case. | Medium | Medium-High |

3.1.7 Understanding of Components

The launch vehicle can be broken into three main sections: the nose cone, the payload, and the motor (top, middle, and bottom sections respectively). The nose cone section is ejected at apogee by a black powder charge. An 18 inch drogue parachute is ejected at apogee. This section is relatively simple so we do not anticipate there being any major risks affecting the success of the project.

The motor section contains the motor which is used to release the payload section, the motor casing, the centering rings, the electronics bay, the two parachutes, the two pvc pipes to hold the parachutes, and the fins. The motor section will deploy two parachutes from the bottom of the rocket, on opposite sides of the motor, which will effectively flip the rocket upside down five seconds after apogee. When the parachutes deploy, the release mechanism will cause the payload section to separate from the motor section. The payload section will continue to descend on the two parachutes until it reaches the ground. The main risks of this section are the release mechanism and the deployment of the two parachutes. The release of the parachutes are a concern due the team’s inexperience with deploying parachutes from this position. The current design should work in theory, but may have to be revisited after some

testing and the subscale launch has occurred. This new method of deploying parachutes will likely lead to some delays.

The mechanism releasing the payload may lead to delays due to its small size and sensitivity. For example, if one of the arms connecting the latch to the threaded rod is bent, the payload section may not be released. This component of the launch vehicle will have to be built and installed with care and may need to be rebuilt if it cannot withstand the force of the launch or landing. This may make it difficult to launch a working model on time.

Finally, the payload section carries the least amount of risk. The primary concerns and potential risks of this section relate to the payload itself (i.e. CDLE and ATMOS). The payload must be able to separate from the motor section, but the main mechanisms controlling this separation are considered to be part of the motor section.

3.1.8 Manufacturing and Testing

Manufacturing and testing of the launch vehicle will take place according to a schedule that focuses on deadlines and launch dates. The subsystems of the launch vehicle will be tested on the ground to ensure proper functionality during flight. This includes testing the release mechanism and the electronics that will deploy the drogue and main parachutes. All circuits will be thoroughly tested on the ground before placed into the subscale or the full scale launch vehicle, allowing for any unforeseen failures. In addition, components, such as fin slots, will be machined by third parties in order to ensure high quality components. Components such as fin slots will be CNC cut by a third party machinist who specializes in CNC machining techniques. The various components of the rocket, such as the ATMOS modules, the CDLE, and the deployment mechanism, will be built separately, with continuous integration meetings between the launch vehicle team, the CDLE team, and the ATMOS team, ensuring that all systems function nominally upon complete assembly of the rocket.

3.1.9 Maturity of Design

The current design of the rocket has gone through approximately ten iterations. With each iteration, our launch vehicle has become safer and more efficient. Most of the major design changes have centered on the deployment of the quadcopter. Initially, the CDLE was going to be deployed using black powder charges at the bottom of the quadcopter. This idea was ultimately abandoned in favor of a mechanical lock system due to concerns about safety and the potential of damage to the quadcopter caused by a black powder detonation. The new mechanical lock system reduces the possibility of damage to the payload. Moreover, in initial designs, the launch vehicle split into three sections during descent. In later stages of the design process, the number of pieces upon descent was increased to four sections. This change simplifies the fabrication procedure for the subscale and the full scale, and it also reduces the number of sections that could potentially fail during flight. We are confident in our current launch vehicle design, as it is significantly simpler and safer than our initial designs. Although our design may change in the time before CDR, our current design contains the most important elements for this project.

3.1.10 Dimensional Drawing

Figure 3.1.10 below is the dimensional drawing for the launch vehicle. The drawing is missing the diameter dimension, previously stated to be 7.5 inches.

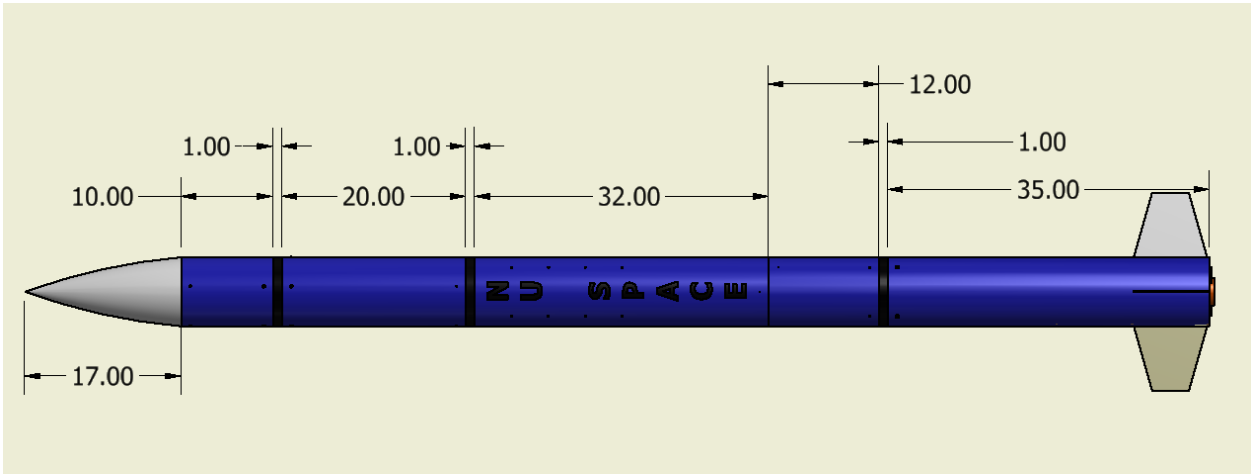


Figure 3.1.10 – Launch vehicle dimensional drawing

3.1.11 Electrical Schematics

Figure 3.1.11 below is a basic electrical schematic of the launch vehicle.

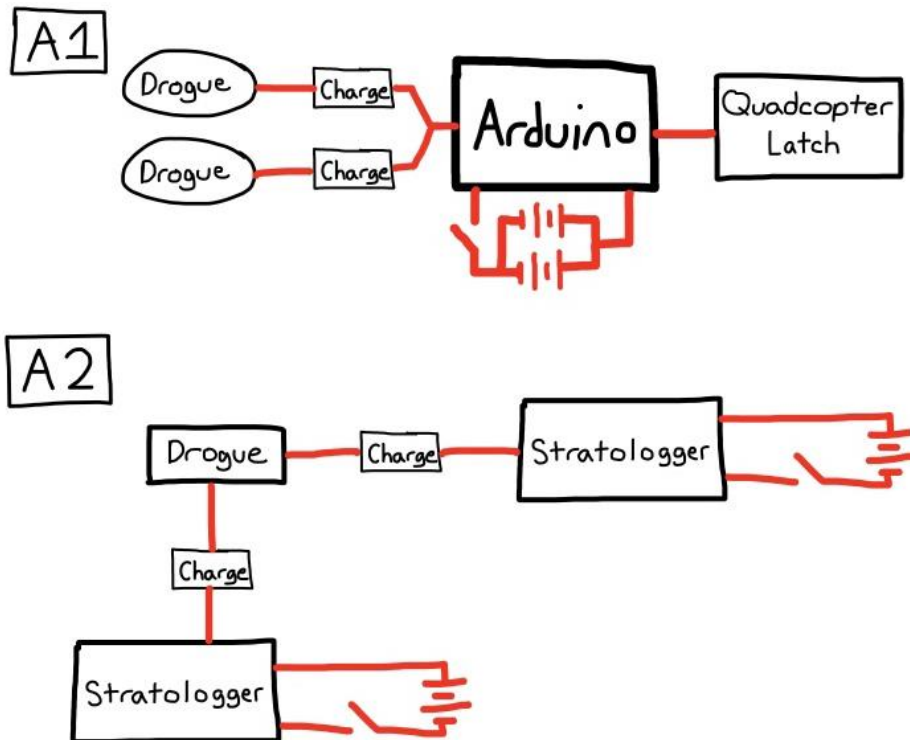


Figure 3.1.11 – Launch vehicle wiring schematic

There are two electronics bays in the launch vehicle to dictate the decent of the two main rocket pieces. The nose cone’s electronics bay consists of a Stratologger, 9V battery, parachute charge, and a radio transmitter. A complete redundant system is wired to the drogue charge in the e-bay. At apogee the Stratologger altimeter fires the drogue charge, which separates the nose of the launch vehicle from the base of the quadcopter, and additionally deploys the parachute.

The aft electronics bay is a more developed system, as it is in charge of deploying the quadcopter at the correct time. An Arduino microcontroller is used along with an IMU to gain telemetry data. The microcontroller is responsible for deploying the drogue and main parachutes, as well as releasing the electromechanical latch holding the quadcopter in place. The Arduino is wired to two 9V batteries in parallel as redundant systems. Each parachute bay also has an additional detonation charge, which is detonated at a later time to ensure that parachutes are deployed for a safe recovery of the launch vehicle.

3.1.12 Mass Statement

The mass statement for the launch vehicle is listed below in Table 3.1.12.

Table 3.1.12 – Launch vehicle mass statement

| Separation | Component | Mass (g) |
|------------|--------------------------------|----------|
| 1 | Nose cone | 485 |
| | Body Tube | 391 |
| | Electronics Bay 1 | 200 |
| | Shock Cord | 133 |
| | Drogue | 34.4 |
| 2 | Body Tube 1 | 782 |
| | Body Tube 2 | 1251 |
| | Bulkhead (2) | 218 |
| | Tube Coupler (2) | 612 |
| | Quadcopter | 5750 |
| | Quadcopter Emergency Parachute | 54 |
| 3 | Separation Mechanism | 150 |

| | | |
|-------|--------------------|----------|
| | Body Tube | 245 |
| | Shock Cord | 11.6 |
| | Main Parachute | 81.5 |
| 4 | Body Tube | 1124 |
| | Tube Coupler | 306 |
| | Fins (4) | 601 |
| | Motor Tube | 50.1 |
| | Motor | 4404 |
| | Engine Block | 1.58 |
| | Inner PVC Tubes | 167 |
| | Drogue (2) | 70.4 |
| | Shock Cord | 8.23 |
| | Centering Ring (3) | 273.6 |
| | Electronics Bay 2 | 150 |
| Foam | 500 | |
| Total | | 18054.41 |

All masses in this estimate were determined with the aid of the vendors that we will be ordering parts from. The dimensions were based off of specifications from Apogee Components and Always Ready Rocketry. This in conjunction with Open Rockets software allowed for the accurate calculation of the masses in each section, reflecting an accurate estimate for the total mass of the rocket. However, this mass statement does not account for hardware or epoxy. Even if there was a mass growth between 25% and 33%, the independent masses that are falling from apogee satisfy the kinetic energy and lateral drift parameters. This percent leeway is visible in the Kinetic Energy Analysis table.

3.2 Recovery System

3.2.1 Analysis

The expected mass of the launch vehicle is 39.91lb (18.1kg) including the motor. This is shown within the mass statement section. The reasoning for the parachute sizes are shown in the simulations of the rocket and the calculations for kinetic energy and drift. The motor section has two PVC pipes that have a cap that the shock cord will go through. The 18 inch

drogue chutes, which are attached to the bulkhead in the motor section, are deployed from these pipes. These drogue parachutes will serve the purpose of positioning the payload section in a favorable position for release and the purpose of getting the section down to a lower height with minimal drift. The payload section is ejected from the motor section (although remaining tethered) 200 meters above the ground. When this occurs, a 48 inch main parachute will be deployed to meet kinetic energy requirements. These will be released at apogee after the nose cone section is removed. The nose cone section will have a drogue parachute of 18 inches. The CDLE will be kept in place by a mechanical lock that will release, ejecting the quadcopter from the payload section, when the quadcopter is in a favorable position for ejection. There is also an emergency parachute on the quadcopter, so that in any emergency scenario which causes the quadcopter to fail, it will still have a controlled descent. Initial calculations have been estimated to find the amount of black powder charge that is required to break the necessary shear pins. The electronics will send signals to begin blasting the black powder charges based upon the altimeter and the projected release heights.

3.2.2 Major Components

Table 3.2.2– Launch vehicle major components

| Component | Purpose | Material |
|--|--|-----------------|
| 18 inch drogue parachute nose cone | To safely get the nose cone to the ground with little drift | Nylon |
| Two (2) 18 inch drogue parachutes connected to motor section | To stabilize ejection of quadcopter | Nylon |
| 38mm PVC pipes | To hold the drogues within the motor sections | PVC |
| 30 inch main parachute | To get the motor and payload sections safely to the ground at a low velocity | Nylon |
| 3-4 recovery beacons (one for each separate section) | To allow the team to recover objects that may disappear from view | Recovery Beacon |

3.3 Mission Performance Predictions

3.3.1 Criteria

The mission performance criteria for the launch vehicle is as follows:

- The launch vehicle must reach of an altitude of 5,280 feet using a motor with no more total impulse than 5,120 Newton-seconds
- The launch vehicle must deploy the payload at an altitude near 5,280 feet
- All sections of the launch vehicle and the payload must fall in a controlled manner and should be recoverable and reusable after launch
- There should be no more than four independent section

3.3.2 Flight Simulations

To predict pertinent information regarding the launch vehicle with respect to time, including apogee, velocities, and lateral distance, simulations were carried out using the Open Rocket software. However, due to the complexities within our systems, including involved and unorthodox safety deployment mechanisms, we discovered that this software is unable to accurately predict terminal velocities and lateral distances of the most complex portion falling: the motor section. Visible in red in Figure 3.3.2.1, the flight paths of the three independent falling pieces, including the quadcopter, are present. It should be noted that during this simulation, the quadcopter was operating under an emergency landing circumstance. While OpenRocket is generally an excellent tool to gain knowledge on a launch vehicle, in this particular case, variables such as terminal velocities and lateral drift did not fluctuate with the addition of new parachute parameters.

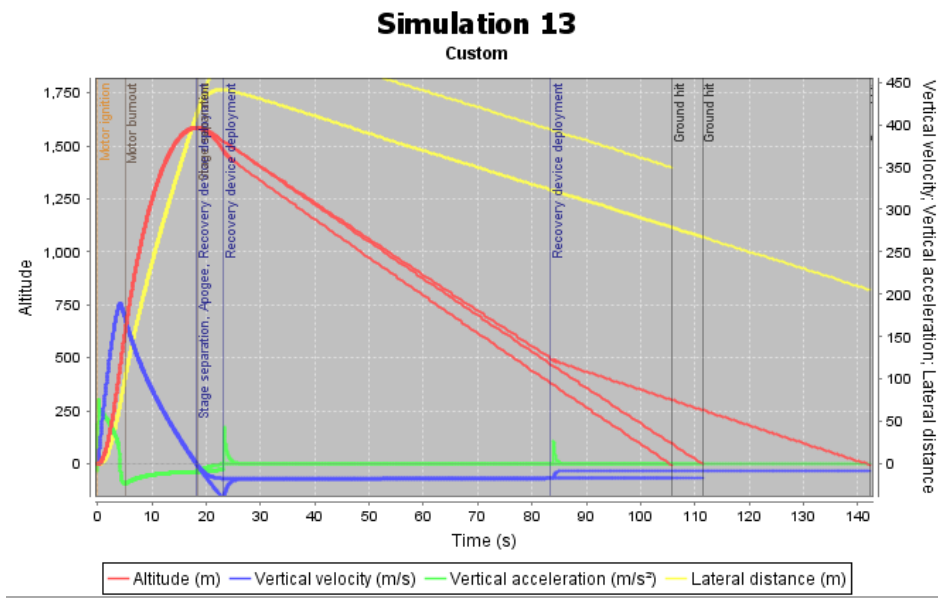
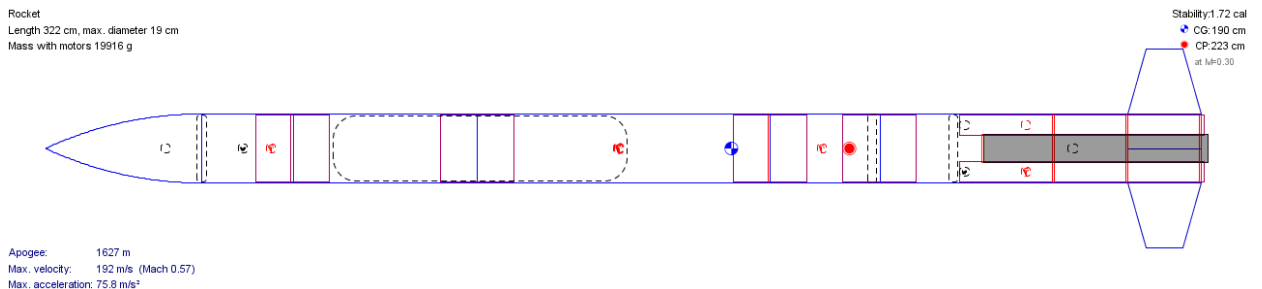


Figure 3.3.2.1 - OpenRocket flight simulation

Thus, a more accurate representation of the simulations were hand-calculated to confirm a safe flight, emphasizing on terminal velocities and lateral drift. These are addressed and determined in the sections below.

3.3.3 Stability Margin

The static margin of stability for the launch vehicle with an L1115 motor is 1.75 calibers. This was determined with the aid of the OpenRocket simulation software, which accounted



for all components and pressures within the launch vehicle. The center of pressure and the center of gravity are depicted in the figure below. The center of gravity (blue) is located at a sufficient distance from the center of pressure, yielding 1.75 calibers.

Figure 3.3.3 – Launch vehicle layout

3.3.4 Kinetic Energy

The kinetic energy can be calculated from the velocity. First, we balanced the forces on the rocket acting in the vertical axis. These forces were weight and drag. The drag equation used was

$$F_D = \frac{1}{2} \rho v^2 A C_D$$

where ρ is the density of air (1.225 kg/m³), A is the sum of the area of the parachutes, and C_D is the coefficient of drag (1.5). Balancing the forces on the rocket gives:

$$ma = mg - \frac{1}{2} \rho v^2 A C_D \text{ thus } v' = g - kv^2$$

Where $k = \frac{\rho A C_D}{2m}$. This differential equation can be solved to give:

$$v(t) = \sqrt{\frac{g}{k} \tanh(t\sqrt{gk})}$$

The calculations tabulated in Table 3.3.4.1 show that the terminal velocities for the nose cone section and motor section fall well within the kinetic energy limit of 75ft-lbs. The calculated apogee is 5278ft, so the height at any time can be calculated by integrating the above equation, and subtracting it from apogee to give

$$h(t) = 5278 - \frac{2}{k} \ln(\cosh(t\sqrt{2gk}))$$

From this equation, the rocket will hit the ground after 238 seconds. The tabulated terminal velocities and their respective kinetic energies are depicted in Table 3.3.4 below.

Table 3.3.4 - Terminal velocities of independent sections of launch vehicle

| Section | Descent Speed (m/s) | Descent Speed (ft/s) | Kinetic Energy (J) | Kinetic Energy (Ft*lbs) |
|-------------------|---------------------|----------------------|--------------------|-------------------------|
| Nose Cone Section | 9.16 | 30.05 | 54.1 | 39.9 |
| Motor Section | 6.09 | 19.90 | 74.2 | 54.72 |

3.3.5 Drift

To calculate drift, specific parameters were first defined. The Coefficient of Drag for all parachutes during descent is 1.5. The assumption of this was that the parachute takes a dome formation. Using the terminal velocities from Table (3.3.4.1), the radial drift displacement (t) was determined, taking wind speed into account. The equation for drift is below:

$$t = \frac{h}{v_t}$$

The wind speeds were incorporated into this calculation by cross multiplying the drift by the wind speed (w).

$$\text{Lateral Drift} = t * w$$

Thus, the lateral drift of the nose cone and motor section for given wind speeds are listed below in Table 3.3.5.

Table 3.3.5.1 - Drift of the independent launch vehicle sections

| Wind Speed (mph) | Nose Cone Drift (m) | Nose Cone Drift (ft) | Motor Section Drift (m) | Motor Section Drift (ft) |
|------------------|---------------------|----------------------|-------------------------|--------------------------|
| 0 | 0 | 0 | 0 | 0 |
| 5 | 391.6 | 1282.8 | 295.7 | 970.1 |
| 10 | 785.0 | 2575.5 | 592.8 | 1944.5 |
| 15 | 1176.6 | 3860.2 | 888.6 | 2915.3 |
| 20 | 1570.0 | 5150.9 | 1185.7 | 3890.1 |

3.4 Interfaces and Integrations

3.4.1 Payload Integration Plan

The overall payload section, consisting of the quadcopter payload and its containment sheath, will be integrated as part of the rocket body. The sheath section, made up of body tubing and the quadcopter release mechanism, will be held onto the motor housing using set screws. This release mechanism will be a spring loaded system. The quadcopter base will be attached to the other end of the sheath using shear pins. The base will also be held onto the nose section using shear pins, acting as the interface between the payload and the nose sections.

The CDLE will be secured to the sheath using three methods. As mentioned, the shear pins will hold the base to the top of the sheath. The arms will be held to the body tube wall using rails, which will also ensure a safe release of the quadcopter and its blades. Finally, a spring

loaded bulkhead will be clamped into a mechanized release system inside the center of the sheath. This clamp will ensure that the quadcopter is locked in place during flight and then eject it using the spring loaded release mechanism at apogee. See Figure 3.4.1 on the next page.

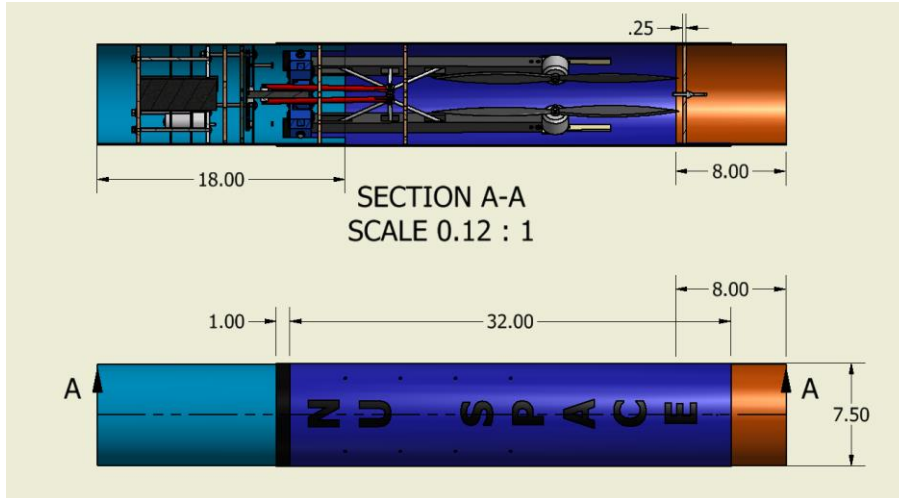


Figure 3.1.2 – Launch vehicle and payload integration

3.4.2 Internal Interfaces

The launch vehicle will consist of three major components; the motor section, the payload section, and the nose cone section. The electronics bay will act as the interface between the motor and the payload sections, attached to both with set screws. As mentioned above, the quadcopter will act as the interface between the payload section and the nose section, instead secured using shear pins. The quadcopter will separate from the nose section using a traditional black powder charge, breaking the shear pins and releasing the parachute. The spring-loaded release mechanism will eject the quadcopter and break the shear pins.

3.4.3 Vehicle and Ground Interfaces

During the flight, the launch vehicle will interface wirelessly with the ground for the purposes of safety. First, we will be placing GPS beacons in all three of the descending sections: the motor section (with payload section), the CDLE, and the nose cone section. The GPS beacons we will be using are Big Red Bees, which we used successfully during last year's student launch. The CDLE is considered an independent section during descent and, though not considered a section of the launch vehicle after it is deployed, it interfaces with the ground more than any other descending section. We will be communicating with the CDLE with a radio operating at 900 MHz. This radio will transmit to a team member's laptop on the ground. The telemetry will include the GPS coordinates, speed, and attitude on the CDLE. This radio will also be responsible for the CDLE "kill switch". If the CDLE were to enter into a flight path that RSO deems a risk the kill switch would be hit; the CDLE would power off and a 36 inch parachute would deploy from its underside. If for any reason during the descent the CDLE should lose radio contact, the CDLE is programmed to continue flight

for 10 seconds in the hopes that it regains contact. If it does not, the emergency parachute will be deployed.

3.4.4 Vehicle and Ground Launch System Interfaces

For the purposes of this section, we will assume that the ground launch system refers to the launch rail and igniter. In the past, we have relied exclusively on standard rail buttons, fitting a 1 inch (1010) launch rail. Due to the size of the launch vehicle we have elected to use large rail buttons for the first time. The large rail buttons we intend to use will fit a 1.5 inch rail (1515). According to Apogee Components, the 1515 rail buttons are ideal for rockets projected to weigh over 10lbs (4.54kg). Two rail buttons will be placed on the launch vehicle positioned so that they straddle the center of mass (located approximately 51 inches up from the base of the launch vehicle).

The launch vehicle will interface with the ignition system with the aid of the electric match that comes with the intended motor. We will insert the electric match into the motor of the rocket and secure it there using the cap on the motor. We will pull the wires apart and attach them to the alligator clips, being sure to keep the two clips far from one another. The launch vehicle will be compatible with the 12 volt direct current firing system provided by the Range Services Provider, as we are using a commercial Cesaroni motor.

3.5 Safety

3.5.1 Preliminary Checklist

Prepare the Quadcopter

1. Preliminary system check
2. Check wiring connections and camera lenses
3. Measure out black powder charges
4. Place black powder into blast caps
5. Cut electronic matches to length
6. Insert electronic matches into blast caps and attach them to terminal blocks
7. Place masking tape over the blast caps
8. Pack emergency parachutes into tubes
9. Connect leads from motor that drives the lead screw to power
10. Drive the lead screw backwards to close the quadcopter
11. Disconnect from power
12. Reconnect the leads of the motor to the quadcopter system
13. Line propellers up vertically
14. Slide quadcopter along rails into the sheath
15. Shear pin the base to the sheath inside the launch vehicle
16. Prepare to attach this section of the launch vehicle to the rest of the body tube

Prepare the Launch Vehicle

1. Open electronic bays
2. Replace batteries, 2 in the back electronic bay and 2 in the front electronic bay for redundancy

3. Check connections in each electronic bay
4. Verify that altimeters power on
5. Turn altimeters off
6. Seal electronic bays
7. Measure black powder charges
8. Place measured charges into blast caps
9. Cut electronic matches to length
10. Insert electronic matches into terminal blocks and screw tight
11. Insert electronic match ends into blast caps
12. Seal blast caps with masking tape
13. Pack the two parachutes in the motor section
14. Attach motor section to bottom electronic bay
15. Insert set screws between sections
16. Attach body tube section to other side of lower electronic bay and set screw together
17. Insert sheath containing the quadcopter into current uppermost section of body tube
18. Shear pin these two sections together
19. Attach top electronic bay to the top of this section and set screw together
20. Attach leads of electronic match to terminal block
21. Pack the drogue chute into the nose cone section
22. Attach the nose cone section to the top of the top electronic bay
23. Shear pin in place
24. Verify that all set screws and shear pins are in place
25. Final visual inspection of launch vehicle
26. Remove motor from cardboard packaging
27. Place motor into aluminum reusable casing
28. Be sure to keep track of motor ignitor attached to outside of tube
29. Place motor casing containing the motor into the motor tube of the launch vehicle
30. Screw closed the aft closure to secure the motor
31. Bring the launch vehicle to RSO for the safety inspection

At the launch pad

1. Bring rail down to horizontal orientation
2. Slide launch vehicle onto rail
3. Return launch rail to upright position
4. Secure launch rail in upright position
5. Only one team member is needed from this point on
6. Insert motor ignitor into motor and verify that it extends to the top of the motor
7. Seal the end of the motor with the yellow cap to keep the ignitor in place
8. Arm the altimeters by turning the rotary switch
9. Use a remote control to power on the quadcopter
10. Final audio inspection to determine status of altimeters
11. Connect leads of motor ignitor to alligator clips which are connected to launch control
12. Verify continuity

3.5.2 Safety Officer

Nathan Kotler
 Safety Officer, Northeastern University AIAA
kotler.n@husky.neu.edu
 (860)817-1178

3.5.3 Preliminary Hazard Analysis

Table 3.5.3 – Preliminary hazards for launch vehicle

| Hazard | Effect | Proposed Mitigations | Likelihood | Severity |
|--|---|---|----------------------|-----------|
| Accidental motor ignition | Potential injury to personnel | Follow MSDS storage requirements. | Extremely Remote | Hazardous |
| Explosive motor failure on launchpad | System damage | Follow MSDS requirements for safe transport and handling of motors. Follow NAR High Power Safety Code and keep personnel at least 200ft from launch pad during launch sequence. | Extremely Improbable | Major |
| Payload does not deploy | None | Correctly measure black powder amounts. Confirm altimeter functionality and igniter connections. | Extremely Remote | No Hazard |
| Payload (CDLE) does not attain stability | Potential injury to spectators and environmental concerns if the CDLE cannot be recovered | Verify that kill switch can remotely disable the CDLE. Verify that backup parachute is properly configured. | Extremely Remote | Major |
| Payload (CDLE) gains too much acceleration | Potential injury to spectators and environmental concerns if the CDLE cannot be recovered | Verify that kill switch can remotely disable the CDLE. Verify that backup parachute is properly configured. Verify that accelerometer is properly configured. | Extremely Remote | Major |
| Payload (CDLE) loses GPS signal to base | Potential injury to spectators and environmental concerns if the CDLE cannot be recovered | Verify that kill switch can remotely disable the CDLE. Verify that backup parachute is properly configured. Verify that GPS is properly configured. | Extremely Remote | Major |
| Sensor falls off the CDLE | Potential Injury to spectators and environmental concerns | Verify that all sensors are properly and securely attached to | Extremely Improbable | Major |

| | | | | |
|--|---|---|----------------------|-----------|
| | if the CDLE cannot be recovered | the CDLE using an appropriate weather and heat resistant epoxy or adhesive | | |
| Kill switch does not activate | Potential injury to spectators and environmental concerns if the CDLE cannot be recovered. Potential damage to landscape or infrastructure from the spinning rotors | Verify that kill switch can remotely disable the the CDLE. Verify that backup parachute is properly configured. Clear evacuation plan with officials. | Extremely Improbable | Hazardous |
| Backup parachute on the CDLE does not activate or malfunctions | Potential injury to spectators and environmental concerns if the CDLE cannot be recovered. Potential damage to landscape or infrastructure from the spinning rotors | Verify that kill switch can remotely disable the CDLE. Verify that backup parachute is properly configured. Correctly measure black powder amounts and confirm altimeter functionality and igniter connections. Clear evacuation plan with officials. | Extremely Improbable | Hazardous |
| Main parachute fails to deploy | Potential system damage | Correctly measure and double check black powder amounts. Confirm altimeter functionality and igniter connections. | Extremely Remote | Minor |
| Drogue parachute fails to deploy | Potential system damage | Correctly measure and double check black powder amounts. Confirm altimeter functionality and igniter connections. | Extremely Remote | Minor |
| Shock cord failure | System damage and potential injury to personnel | Inspect shock cord thoroughly before flight. | Extremely Improbable | Major |

3.5.4 Environmental Concerns

The environmental concerns regarding our launch vehicle fall into two broad categories: our launch vehicle's effect on the environment and the environment's effect on our launch vehicle.

Among our launch vehicle's effects on the environment, the most prominent concern is the ecotoxicity of the launch vehicle motor. We will be using an L1115 motor manufactured by Cesaroni Technology which does not have any published ecotoxicity data on their Pro 75 Material Safety Data Sheet. However, we will still be taking precautions to reduce our impact on the environment, including placing flame retardants beneath the launch pad to avoid heat damage to the surrounding environment and using a metal launchpad to reduce the risk of a fire. After the flight, we will dispose of the motor and the igniter according to the disposal considerations outlined in the appropriate MSDS.

In addition to the concerns with the motor, we must also consider that we do not want to disturb the environment by leaving behind pieces of the launch vehicle or the payloads. To avoid this, the sections of our launch vehicle are designed to stay intact during descent. We

will also be implementing drogue parachutes in conjunction with the main parachutes to ensure that the launch vehicle sections descend at reasonable velocities and to reduce the probability that pieces break off and get lost in the environment upon impact. The CDLE, on the other hand, is designed to be safely controlled from the ground to a gentle landing. However, in the event that this becomes infeasible during any stage of the descent, we will activate the backup parachute with the kill switch. This should ensure that the CDLE does not break into pieces upon impact. In the extremely unlikely event that the CDLE loses radio contact with the team member monitoring it from the ground the backup parachute will be activated. This feature would prevent the CDLE from damaging the environment even if radio communication is lost. Lastly, we will ensure that all components of our launch vehicle and payload are accounted for upon completion of the launch.

During the flight, the CDLE raises some environmental concerns as well. The spinning rotors pose the risk of damaging surrounding infrastructure, disrupting the wildlife, and potentially injuring flying birds or insects. For this reason we will be implementing a GPS tracking system to maintain constant location data on the CDLE. We will also be implementing a “kill switch” that will power off the motor if the CDLE loses signal to the base or becomes too difficult to control from the ground. This kill switch can also be triggered manually from the ground. This will greatly reduce the risk of the CDLE colliding with or damaging the surrounding environment or harming the wildlife. In addition, if we cannot safely land the CDLE at a manageable speed, we will deploy a backup parachute that will ensure the CDLE does not damage the surrounding landscape upon landing.

On the flip side, environmental factors may have a profound effect on our launch vehicle, the greatest of which is the weather. Our launch vehicle will be made out of blue tube, a material that is not 100% weather resistant. For this reason all forms of precipitation, including, but not limited to, rain, snow, sleet, and hail, could have an effect on our launch vehicle. Water, in any form, could compromise the electronics system in the launch vehicle and on the CDLE, as well as the other elements of the body. Strong force winds carrying dust and other particulate matter may also compromise the electronics systems in addition to greatly affecting the trajectory of the CDLE and the launch vehicle. To reduce the weather’s effect on the launch vehicle, we will try our best to avoid launching during inclement weather or if the local weather data suggests that there will be an impending storm. Lastly, snow and water on the ground could present concerns for the same reasons as precipitation. To avoid this we will store our launch vehicle in a dry area and check for damp sections of earth before resting our rocket on the ground.

4. PAYLOAD CRITERIA

4.1 Selection, Design, and Verification - CDLE

4.1.1 System Review

The payload, referred to as the CDLE, is a custom quadcopter that integrates both the science and engineering payloads into a single functional unit. The CDLE integrates the ATMOS systems into its own frame and allows for the ATMOS to interface with the ground control station independently of the Pixhawk Flight Controller that controls the flight logic for the CDLE. The CDLE works as a deployable mechanism from the rocket, capable of rapidly

separating from the launch vehicle and deploying its own means of powered and controlled descent. Once deployed, the CDLE will initiate an autonomous landing sequence, allowing for ATMOS to collect scientific data as it completes a powered descent towards a predefined landing site. The main goal of this experiment is to soft land the CDLE in a predefined location without losing control, communication, or power.

When the CDLE is ejected from the rocket, it will be stowed in its folded and locked position. In order to power up motors and begin descent, the CDLE must unfold and lock its arms. We have designed the CDLE Arm Release Actuator (CARA) to complete this task. The CARA uses a motor to power a lead screw, which translates a threaded bearing up the lead screw, and uses a linkage to push the arms down.

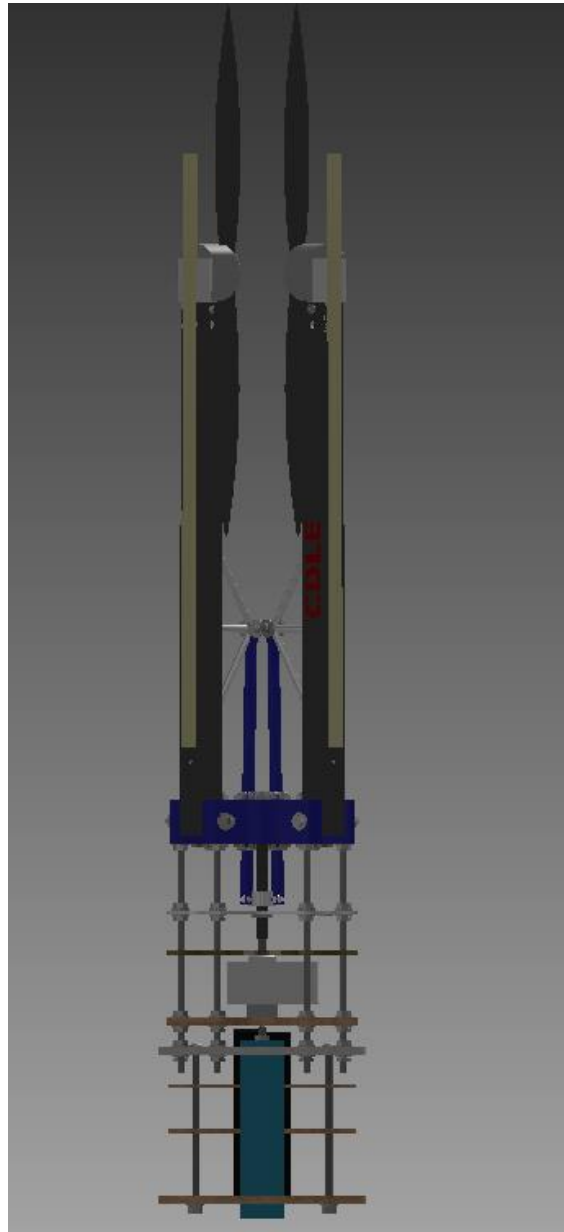


Figure 4.1.1.1 – CDLE deployment system side view

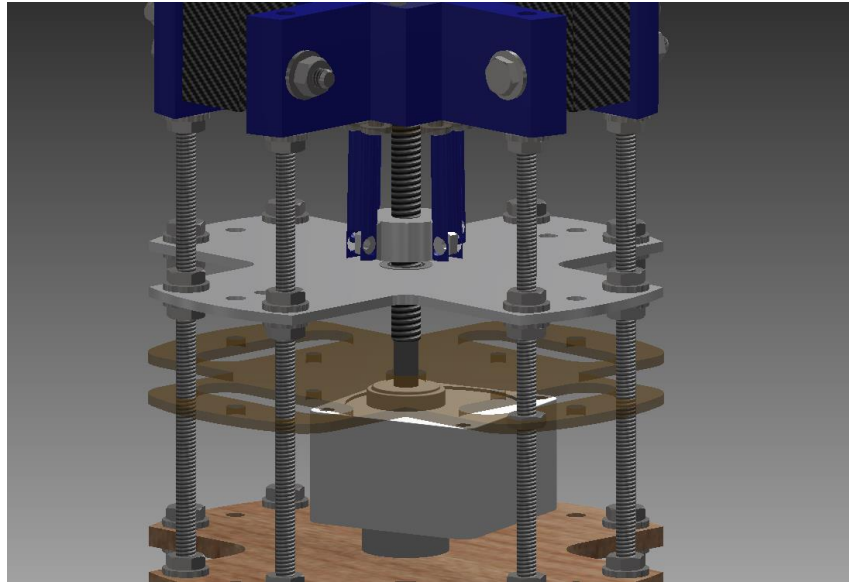


Figure 4.1.1.2 – The CARA

The CARA is powered by a KDE 2306 XF-2050 motor, rated for 2050 revs/volt. At approximately 12 volts, the motor will spin at 24600 rpm. The output of this motor powers a planetary gearbox with a ratio of 1:30. The gearbox will output at 820 rpm, causing the threaded bearing to move up the shaft, and actuating the arm linkage.

The motor and gearbox will both be mounted to a laser cut motor mount plate. This motor mount plate will sit directly beneath the electronics bay and it will be attached to the rest of the CDLE via a series of 8¹/₄-20 aluminum threaded rods.

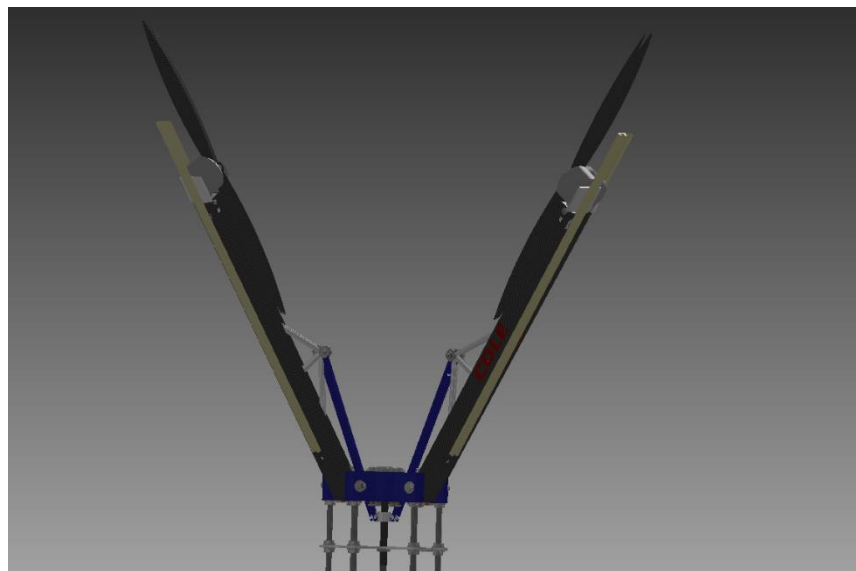


Figure 4.1.1.3 – CDLE arm deployment

The bearing will continue until the arms are fully deployed. Once they are fully deployed, a mechanical latch will lock them in place. This whole process is projected to take approximately 4 seconds, which is about half of the “10 Seconds of Chaos”.

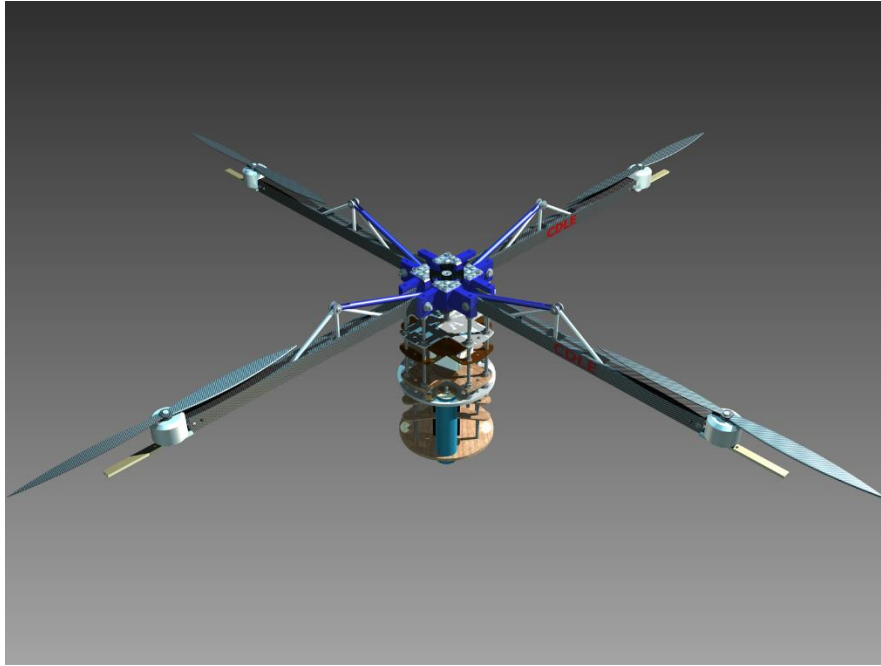


Figure 4.1.1.4 – Deployed CDLE payload

The arm deployment and locking system consists of a series of struts attached to a linearly actuating bearing that will be driven by a lead screw. The lead screw will be driven by a brushless DC motor which drives a planetary gearbox. The planetary has a gear ratio of 30:1 which reduces the RPM of the output, but steps up the torque to 2.6lb/in. In order to make the arms pivot a full 90 degrees, the bearing only needs to travel approximately 3 inches up the $\frac{3}{8}$ x 16 leadscrew. The arms will be secured in place by a mechanical latch, which will engage once the arms have reached their deployed position, and will hold them there for the duration of flight operations.

We have selected the KDE4014XF-380 as the primary motor for the CDLE. With 15.5 inch diameter propellers, the manufacturer has reported that each motor will produce a maximum thrust of 6.97lb per motor. More importantly, at 62.5% power, the motors will output approximately 3.31lb of thrust per motor. With 4 motors on the CDLE, this gives us a total of 27.88lb of thrust at maximum power, and a total of 13.24lb of thrust at 62.5%. Since CDLE weighs 13.2lb, we are able to approximately hover with CDLE at 62.5%, which is important for the maneuverability and control of the system.

The battery we have selected to power the CDLE is a Turnigy 5000mAh 6S battery. This is a 22.2 volt battery capable of a continuous maximum discharge of 200 amps. This will give us a maximum of 5 minutes of flight time with the motors drawing an average of 44 amps, which is 75% motor power. This battery weighs 1.9 lb.

Table 4.1.1.1 – CDLE specifications

| | |
|------------------|-------------------------------|
| Motor | KDE4014XF-380 |
| Type | Brushless DC |
| Voltage | 22.2 - 29.6 V DC |
| RPM/Volt | 380 |
| Maximum Amperage | 36+A |
| Magnetic Poles | 24 |
| Shaft Diameter | 4mm |
| Motor Diameter | 46.5mm |
| Weight | 215g with propellers and nuts |

Table 4.1.1.2 – CDLE power supply specifications

| | |
|--------------|-------------------------|
| Battery | Turnigy 5000mAh 6s |
| Type | Lithium Polymer Battery |
| Battery Life | 5000mAh |
| Voltage | 22.2 (6S) |

Table 4.1.1.3 – CDLE propeller specifications

| | |
|-----------------|-------------------------|
| Propeller | KDE-CF155-DP-Dual Blade |
| Diameter | 15.5" |
| Material | Carbon Fiber |
| Thrust at 62.5% | 3.31lbs |

The CDLE will be constructed out of a variety of materials. The main body of the quadcopter will be machined out of Delrin plastic. This ensures structural integrity of the chassis while minimizing the total weight of the body. To simplify the manufacturing process, the chassis will be constructed in four sections and lined up by inserting an interference pin in the corners. The four sections will be permanently secured with screws and brackets. Plates within the body tube will be included to support electronics as well as the sensors for ATMOS. These will be fabricated out of wood, as they are not load bearing and will minimize the weight of the CDLE.

The arms of the quadcopter will be constructed of 1 inch by 1 inch square carbon fiber tubing. They will be secured to the body with a ¼ inch bolt, which will act as the pivot point. The arms will also be secured to the body by a series of struts that aid in the deployment process and then provide structural support. A truss structure will be incorporated onto the top of each arm to add strength to the arm, and to give a more efficient moment arm for the deployment procedure. These will be made using ¼ inch aluminum rods, as they will need to be able to withstand the force of the deployment bearing while staying lightweight.

4.1.2 Subsystem Descriptions

The success of the scientific payload depends on the reliability and speed with which the quadcopter can deploy its arms into a ready state. A lead screw pushes on the aluminum trusses to extend the arms. A brushless motor running at 43200 RPM transfers power through a 30:1 gearbox that in turn spins the lead screw at 1440 RPM. The gearbox converts the .087 lb-in (.1 kg-cm) torque of the motor into a 2.6 lb-in (3 kg-cm) moment applied on the 3/8 16 lead screw. A 1018 carbon steel precision ACME threaded rod is used, along with a 660 bronze drive nut that connects to the trusses. A coefficient of kinetic friction $\mu_k = .10$ is approximated from an average of material studies on carbon steel and bronze interactions. A lead screw moment equation is used to find the applied upward force on the drive nut.

$$M = r_{avg}F * \tan(\theta_k + \alpha) \quad [1]$$

$$\theta_k = \arctan(U_k) \quad [2]$$

$$.1 = \arctan(.1) \quad [2a]$$

$$\alpha = \text{thread pitch angle} = \arctan\left(\frac{P}{2\pi r}\right) \quad [3]$$

$$.02955 = \arctan\left(\frac{.0625}{2\pi(.3365)}\right) \quad [3a]$$

$$\text{Solving for 1: } 2.6 \text{ lb in} = F_y * \tan(.1 + .02955) \rightarrow F_y = 20 \text{ lb} \quad [1a]$$

The result for the system is that the lead screw turn with a moment of 2.6 lb-in and will exert a force of 22lb on the drive screw. The maximum force that the arms will experience is 2.1lbs when fully extended and falling at a terminal velocity of 115 ft/s (35m/s). The force translates to 8.4lb on the lead screw, which impedes the motion of the arm deployment in a worst case

scenario. In the anticipated event that the quadcopter is not oriented normal to the ground during deployment, this means that the experienced force will be less than 8.4lbs. The 22lb maximum drive force of the lead screw allots for a safety factor of just over 2.5 times. This force is experienced when the arms are in the process of deploying in free fall, and the absolute maximum will occur if the quadcopter is oriented right side up, as the air will press against the arms, impeding their motion. That being said the deployment orientation of the quadcopter out of the rocket is not guaranteed, and it is possible that the arms will begin to deploy while the quadcopter is upside down; which will actually reduce the force on the arms, and assist in their deployment. Additionally the 8.4lb force is based on the condition that the arms are very nearly fully deployed, while in actuality the projected area of the arms relative to the velocity vector is increasing over time to the maximum, meaning that the force will be much less than the maximum for the majority of the arm deployment.

The drive nut has a stroke length of 3 inch, and with a thread per inch count of 16, the lead screw will have to turn 48 times to fully extend the arms. To achieve a 2 second deployment, the lead screw will have to spin at 24 RPS (1440 RPM), and the motor will spin at 43200 RPM with the 30:1 gear ratio. A brushless motor is used as it can spin at the required RPM and provide at least 100g-cm (1.388 oz-in) of torque. Even though the brushless motor has low torque, the fast speed and the high gear ratio allow it to provide the necessary moment to power the lead screw under maximum load.

4.1.3 Performance Characteristics

The deployment method out of the rocket does not guarantee the orientation in which the quadcopter will be in. In the event that the quadcopter is traveling antinormal to the earth, the arms will want to retract back into a closed position; to safeguard the deployment, ratchets are affixed to the top and bottom of the lead screw to ensure one way rotation of the rod. Once the lead screw has fully extended the arms and the nut has traveled the 3" stroke length, the nut will spin itself off of the lead screw threads; preventing the arms from retracting once deployed. Additionally each arm clicks into a one way mechanical lock mounted on the undercarriage of the quadcopter that secures them in a deployed state; ensuring that the arms are ridged when deployed, and cannot retract back into a semi-deployed state, additionally making sure that the lead screw is not responsible for holding the arms in place while the quadcopter is in flight.

The arms are made of 1" x 1" hollow carbon fiber rectangular prisms, with a wall thickness of 5/100" and are 18" long. The hollow bars help to reduce the overall mass, and gives the wires a place to sit where they will not interfere with the locking mechanism or other arms. An opening is cut on each arm near the pivot point, serving as a connection point for the trusses and an escape hatch for the wires running through the arms. A small rail is mounted on the underside of each arm that allows the quadcopter to slide out of the rocket sheath in a safe, straight, and controlled manner. The aluminum trusses are used to translate the linear motion of the driving nut into an angular force that actuates the arms. Each arm pivots from the Delrin mounting bracket that binds the arms to the rest of the quadcopter undercarriage.

The conglomeration of electronics systems is mounted on the quadcopter via mounting brackets cut into the structural rings underneath the main body. Once the quadcopter detects

that it has left the sheath of the rocket and one second has passed to allow for clearance, the lead screw motor will spin until the microcontroller gets confirmation that the arms are locked into place via a switch. Allowing the lead screw to dislodge itself from the threading allows for the motor to continue to turn after securing the arms, without driving the arms past their 90° deployment point; a mechanical precaution safeguarding against software failure.

Threaded 1/4 – 20 rods are secured into the mounting bracket, and extend through the undercarriage. ¼ plywood disks are secured to the threaded rods and serve as mounting locations for the ATMOS sensors, flight computers, GPS and radio beacons, batteries, and emergency parachute tubes. The ATMOS system is an independent subassembly that serves as the science payload for the quadcopter. There is also an emergency isolated failsafe circuit complete with an IMU built in which allows for independent detonation of the emergency parachutes if it senses a problem with the flight. Additionally the quadcopter’s flight computers can abort the mission in an emergency scenario, which is the preferred method as it will have the ability to deactivate the propellers if they are spinning, preventing the blades from tangling with the parachute.

To summarize: the CDLE will act as the primary scientific payload. The overall system will be a deployable quadcopter containing four major, mechanical subsystems: a lead screw for arm deployment, the motors and propellers, the landing gear, and the emergency recovery system. The performance characteristics of the system and subsystems are mathematically evaluated to determine possible outcomes given a variety of situations. Failure criteria and optimization are also considered.

The CDLE performance relies on the aerodynamic analysis to determine the velocity profile. A general force balance equation is used to characterize the flight of the CDLE payload.

$$ma = F_{Lift} + F_{Drag} - mg \quad [4]$$

$$F_{Drag} = \frac{1}{2} \rho C_D A v^2 \quad [5]$$

$$m \frac{dy^2}{dt^2} = F_{Lift} + \frac{1}{2} \rho C_D A \left(\frac{dy}{dt} \right)^2 - mg \quad [6]$$

The solution to this differential equation has been attempted, but the solution and optimization require more grunt calculation to derive proper values. This equation will be evaluated further in future design review documentation. Thus far, Wolfram Alpha has been used to attempt the solution:

Wolfram Alpha →

$$y(t) = \frac{-m \log\left(\cos\left(\frac{\sqrt{a} t \sqrt{F-gm}}{m} - \cos^{-1}\left(-\frac{\sqrt{F-gm}}{\sqrt{2500a+F-gm}}\right)\right)\right) + m \log\left(-\frac{\sqrt{F-gm}}{\sqrt{2500a+F-gm}}\right) + 1300a}{a}$$

The CDLE will be using four 15.5 inch dual propeller blades to generate the lift force powered by a 5000mAh battery. The specification sheets for these three components are displayed below.

| MOTOR VERSION | VOLTAGE [V] | PROPELLER SIZE | THROTTLE RANGE | AMPERAGE [A] | | POWER INPUT [W] [hp] | | THRUST OUTPUT [g] [N] [lb] | | | RPM [rev/min] | EFFICIENCY [g/W] [lb/hp] | |
|---------------------------|-------------------------|---|----------------|-------------------|-------------------|----------------------|------|----------------------------|-------|------|---------------|--------------------------|--------------------|
| | | | | (LOWER IS BETTER) | (LOWER IS BETTER) | (LOWER IS BETTER) | (hp) | (HIGHER IS BETTER) | (N) | (lb) | | (HIGHER IS BETTER) | (HIGHER IS BETTER) |
| KDE4014XF-380 (380Kv, D5) | 22.2V (6S) 25.2V MAX | 15.5" x 5.3 KDE-CF155-DP DUAL-BLADE | 25.0% | 0.9 | 19 | 0.03 | 320 | 3.14 | 0.71 | 2340 | 16.84 | 27.69 | |
| | | | 37.5% | 2.1 | 46 | 0.06 | 600 | 5.88 | 1.32 | 3300 | 13.04 | 21.44 | |
| | | | 50.0% | 4.0 | 88 | 0.12 | 1020 | 10.00 | 2.25 | 4200 | 11.59 | 19.06 | |
| | | | 62.5% | 6.8 | 150 | 0.20 | 1500 | 14.71 | 3.31 | 5100 | 10.00 | 16.44 | |
| | | | 75.0% | 10.4 | 230 | 0.31 | 2030 | 19.91 | 4.48 | 5880 | 8.83 | 14.51 | |
| | | | 87.5% | 15.4 | 341 | 0.46 | 2690 | 26.38 | 5.93 | 6720 | 7.89 | 12.97 | |
| | | | 100.0% | 19.5 | 432 | 0.58 | 3160 | 30.99 | 6.97 | 7260 | 7.31 | 12.03 | |
| | 25.2V MAX | 15.5" x 5.3 KDE-CF155-DP TRIPLE-BLADE | 25.0% | 1.0 | 22 | 0.03 | 350 | 3.43 | 0.77 | 2240 | 15.91 | 26.15 | |
| | | | 37.5% | 2.7 | 59 | 0.08 | 730 | 7.16 | 1.61 | 3200 | 12.37 | 20.34 | |
| | | | 50.0% | 5.0 | 111 | 0.15 | 1240 | 12.16 | 2.73 | 4060 | 11.17 | 18.37 | |
| | | | 62.5% | 8.5 | 187 | 0.25 | 1800 | 17.65 | 3.97 | 4880 | 9.63 | 15.82 | |
| | | | 75.0% | 12.8 | 283 | 0.38 | 2390 | 23.44 | 5.27 | 5600 | 8.45 | 13.88 | |
| | | | 87.5% | 19.2 | 425 | 0.57 | 3140 | 30.79 | 6.92 | 6400 | 7.39 | 12.15 | |
| | | | 100.0% | 23.6 | 523 | 0.70 | 3620 | 35.50 | 7.98 | 6840 | 6.92 | 11.38 | |
| KDE5215XF-330 (330Kv) | 22.2V (6S) 25.2V MAX | 18.5" x 6.3 KDE-CF185-DP DUAL-BLADE | 25.0% | 1.9 | 42 | 0.06 | 550 | 5.39 | 1.21 | 2280 | 13.10 | 21.53 | |
| | | | 37.5% | 3.6 | 79 | 0.11 | 980 | 9.61 | 2.16 | 3060 | 12.41 | 20.39 | |
| | | | 50.0% | 6.8 | 151 | 0.20 | 1670 | 16.38 | 3.68 | 3900 | 11.06 | 18.18 | |
| | | | 62.5% | 11.6 | 257 | 0.34 | 2480 | 24.32 | 5.47 | 4740 | 9.65 | 15.86 | |
| | | | 75.0% | 18.5 | 411 | 0.55 | 3480 | 34.13 | 7.67 | 5640 | 8.47 | 13.92 | |
| | | | 87.5% | 28.4 | 629 | 0.84 | 4620 | 45.31 | 10.19 | 6420 | 7.34 | 12.08 | |
| | | | 100.0% | 37.0 | 821 | 1.10 | 5520 | 54.13 | 12.17 | 7020 | 6.72 | 11.05 | |
| | 25.2V MAX | 18.5" x 6.3 KDE-CF185-DP TRIPLE-BLADE | 25.0% | 2.2 | 48 | 0.06 | 600 | 5.88 | 1.32 | 2000 | 12.50 | 20.55 | |
| | | | 37.5% | 4.4 | 97 | 0.13 | 1160 | 11.38 | 2.56 | 2880 | 11.96 | 19.66 | |
| | | | 50.0% | 8.7 | 193 | 0.26 | 2020 | 19.81 | 4.45 | 3800 | 10.47 | 17.21 | |
| | | | 62.5% | 14.9 | 329 | 0.44 | 2980 | 29.22 | 6.57 | 4600 | 9.06 | 14.89 | |
| | | | 75.0% | 23.5 | 521 | 0.70 | 4110 | 40.31 | 9.06 | 5360 | 7.89 | 12.97 | |
| | | | 87.5% | 35.9 | 797 | 1.07 | 5400 | 52.96 | 11.90 | 6160 | 6.78 | 11.14 | |
| | | | 100.0% | 46.9 | 1040 | 1.39 | 6460 | 63.35 | 14.24 | 6740 | 6.21 | 10.21 | |

Note: performance chart provided under the test conditions listed below. Measurements taken under alternate conditions will affect the final results.
 Location: KDE Direct Dynamometer (Bend, Oregon)
 Altitude: 3730 ft (1137 m)
 Pressure: 30.3 inHg (1026 hPa)
 Temperature: 72 °F (22 °C)
 Humidity: 35% (Relative)

Performance data for KDE-CF155-TP Propeller Blades, 15.5

Figure 4.1.3.1 – CDLE propeller specifications chart

Table 4.1.3.1 – CDLE motor specifications chart

| Full Specifications: | |
|----------------------------------|----------------------------------|
| Kv | 380 RPM/V |
| Maximum Continuous Current* | 36+ A (180 s) |
| Maximum Continuous Power* | 1065+ W (180 s) |
| Maximum Efficiency | > 91% |
| Voltage Range | 16.8 V (4S) - 33.6 V (8S) |
| I _o (@10V) | 0.5 A |
| R _m (Wind Resistance) | 0.075 Ω |
| Stator Poles | 18 (18S24P) |
| Magnetic Poles | 24 (18S24P) |
| Bearings | Triple, 685ZZ/625ZZ |
| Mount Pattern | M4/3 x φ25 mm, M3/2.5 x φ32 mm |
| Stator Class | 4014, 0.2 mm Japanese |
| Shaft Diameter | φ4 mm (φ5 mm Internal) |
| Shaft Length | 5.5 mm |
| Motor Diameter | φ46.5 mm |
| Motor Length | 32 mm |
| Motor Weight | 160 g (215 g with Wires/Bullets) |
| Propeller Size | Up to 18.5" (16" Maximum on 8S) |
| Motor Timing | 22° - 30° |
| ESC PWM Rate | 16 - 32 kHz (600 Hz) |

Table 4.1.3.2 – CDLE battery specifications chart

| | |
|---------------------|------|
| Capacity(mAh) | 5000 |
| Config (s) | 6 |
| Discharge (c) | 40 |
| Weight (g) | 836 |
| Max Charge Rate (C) | 5 |
| Length-A(mm) | 150 |
| Height-B(mm) | 49 |
| Width-C(mm) | 52 |

The propeller and motor subsystem of the CDLE were chosen to supply a lift force equal to or greater than the total weight of the CDLE system while operating at 60% throttle. Referring to the specification table, 62.5% throttle provides a thrust/lift force of 3.31lb per propeller and draws 6.8A. The performance calculations:

$$BatteryLife = \frac{Capacity}{CurrentLoad} * 0.7 = \frac{5000mAh}{4 * 6800mA} * 0.7 = 0.184hr * \frac{60min}{hr} = 11.03min$$

$$F_{Lift,62.5\%} = 4 * 3.31lb = 13.24lb$$

The emergency recovery system uses two 44 inch parachutes for the CDLE emergency recovery system. This configuration has two major performance concerns: the descent velocity and the maximum drift. These calculations included a few assumptions. The maximum wind speed is 20mph and does not affect the terminal velocity. Assuming the worst case scenario, the emergency system has to be implemented immediately after deployment. The drag coefficient and projected area of the parachute are obtained from manufacturer specifications listed below.

44" ANGEL PARACHUTE



- 🔥 Part Number (PN): 29135
- 🔥 Qty per pack: 1
- 🔥 Material: Silicone-coated rip-stop nylon
- 🔥 Weight: 283.5 g (9.92 oz)
- 🔥 Carrying Capacity: 4 to 9 lbs
- 🔥 Parachute Shape: Skirted Circular
- 🔥 Descent Rate (Cd): 1.87 (Cd)
- 🔥 Shroud Line Length: 44" (111.76 cm)
- 🔥 Parachute Area: 21.1ft² (3038.4in², 1.945m²)
- 🔥 Manufactured by: LOC Precision Rocketry

Figure 4.1.3.2 – Emergency parachute for the CDLE

In the worst case scenario, the descent velocity is equal to the terminal velocity of the CDLE with the emergency parachutes deployed. The calculations for this problem:

$$mg = F_{Drag,tot} = \frac{1}{2} \rho C_D A v^2$$

$$mg = F_{Drag,1} + F_{Drag,2} = 2 \left(\frac{1}{2} \rho C_D A v^2 \right)$$

$$v_T = \sqrt{\frac{mg}{\rho A C_D}} = \sqrt{\frac{4mg}{\rho \pi D^2 C_D}} = \sqrt{\frac{4 * 13lb * 32.2 \frac{ft}{s^2}}{0.0765 \frac{lb}{ft^3} * \pi * (3.67ft)^2 * 1.87}} = 16.6 \frac{ft}{s}$$

$$E_K = \frac{1}{2} m v^2 = \frac{1}{2} * \frac{13lb}{32.2 \frac{ft}{s^2}} * \left(16.6 \frac{ft}{s} \right)^2 = 55.6 ft * lb$$

The total kinetic energy at impact is 55.6 ft-lbs, which falls under the allotted 75ft-lbs.

The calculations for the maximum drift are as follows:

$$t_{descent} = \frac{height_{max}}{v_{descent}}$$

$$r_{drift} = windspeed * t_{descent} = \frac{20miles}{hr} * \frac{5280ft}{miles} * \frac{1hr}{3600s} * \frac{5280ft}{16.6\frac{ft}{s}} = 8614ft$$

This exceeds the allowed, maximum drift radius. In order to meet the requirements for drift radius, the maximum height that the emergency parachute can be deployed is:

$$height_{max} = \frac{r_{descent} * v_{descent}}{windspeed} = \frac{2500ft * 16.6\frac{ft}{s}}{20mph * \frac{5280ft}{miles} * \frac{1hr}{3600s}} = 1415ft$$

4.1.4 Verification Plan

We currently have computer generated models of each component and have done hand calculations to verify forces that determine and limit certain aspects of our design; including material, motors/propellers, and other components we will use. Using these, we will create a prototype to be tested in a controlled setting.

Table 4.1.4 – CDLE verification plan

| CDLE Section | Payload Requirement | Design Feature to Satisfy Requirement | How Requirement will be Verified |
|---------------------|---|--|--|
| Mechanical | The CUDL will fit within a 32in long by 7.5” diameter cylinder sheath | The arms of the quadcopter are designed to pivot, so that while the arms are in the upward position, quadcopter fits inside the rocket | CAD models of both the quadcopter and launch vehicle show that the quadcopter fits comfortably within the launch vehicle. |
| Mechanical | The CUDL will be deployed when the rocket is at apogee | During launch, clamps will hold the quadcopter in place. At apogee, the clamps will unlock the quadcopter, and a spring will push the quadcopter out of the sheath and an acceptable distance from the other launch vehicle components | We will create a prototype that we will test in a controlled setting, taking into account undetermined forces and a factor of safety |

| | | | |
|---------------------|---|--|--|
| Mechanical | During deployment, the CUDL will be ejected from the rocket in a smooth and predictable unveiling | Attached to each arm will be slide buttons that slide along linear slides, guiding the quadcopter out of the payload chamber in a predictable unveiling | We will create a prototype that we will test in a controlled setting, taking into account undetermined forces and a factor of safety |
| Mechanical | After deployment, the CUDL arms will unfold and lock in position | Lead screw placed in the center of the arms, with the arms attached to a bearing. As the lead screw turns and the bearing moves up, the arms will pivot downward until they are in position, at which a separate locking mechanism will lock the arms in place | We will create a prototype that we will test in a controlled setting, taking into account undetermined forces and a factor of safety |
| CDLE Section | Payload Requirement | Design Feature to Satisfy Requirement | How Requirement will be Verified |
| Software | Stabilize flight within 10 seconds of deployment (auto-level) | CDLE will use PX4 stabilization routine to automatically manipulate itself into the proper orientation | Run extensive virtual simulation (with various deployment conditions) and test outdoors |
| Software | Fly at 50% for approx. 120 to 400 seconds battery life | The 5000mAh battery will be able to fly 400s during the quadcopter's descent while collecting ATMOS data | Using hand calculations, we will determine the power needed to stabilize the quadcopter and the power required by the motors to slow and control descent until landing |
| Mechanical | Electronics must be shielded from recovery system | Emergency parachute on an independent circuit that will be shielded from all other electronics | We will create a prototype that we will test in a controlled setting, where we will test the reliability of the shielding |
| Mechanical | Emergency uncontrolled descent protocol | An emergency parachute will be added to the bottom of the electronics console in the event of catastrophic failure or uncontrolled descent. A flight kill switch will | We will create a prototype that we will test in a controlled setting, taking into account undetermined |

| | | | |
|------------|---|---|--|
| | -uncontrolled descent under 1000ft -speed more that \diamond under 1000ft | automatically kill all electronics except for the locator beacon, and deploy the emergency parachute | forces and a factor of safety |
| Mechanical | Payload recoverable and reusable | The center lead screw will be able to pivot up and down, and the locking mechanism will be able to unlock manually. All materials used in the quadcopter will be made from materials high strength materials such as carbon fiber and Delrin, which should be able to withstand impact in the event of an emergency landing or collision with any falling parts of the launch vehicle | We will create a prototype that we will test in a controlled setting, taking into account undetermined forces and a factor of safety |

4.1.5 Preliminary Integration Plan

CDLE will be integrated with the Launch Vehicle on two fronts.

The bottom of the CDLE will be screwed into the upper parachute section with #2-56 Nylon screws. These screws will be sheared at apogee when the first ejection charge goes off in the upper section of the launch vehicle. The upper section of the launch vehicle will then separate from the bottom of the CDLE.

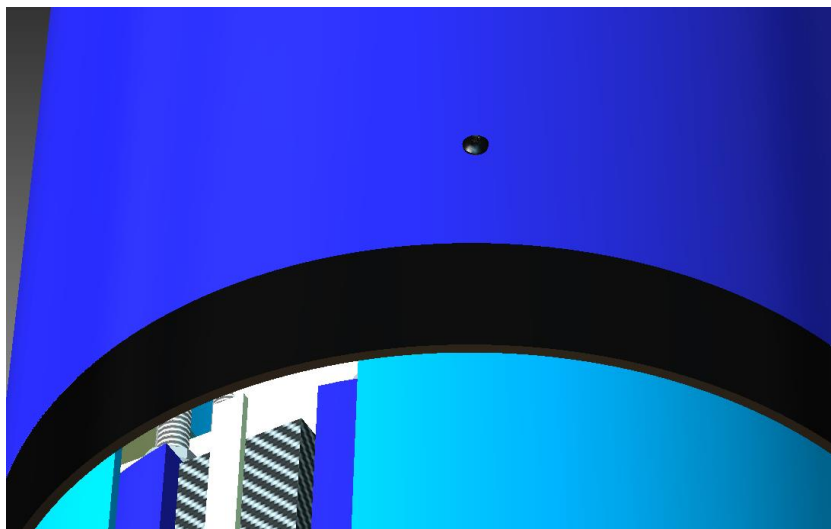


Figure 4.1.5.1 – CDLE shear pin hole

Separating the other section of the rocket (the motor section and CDLE sheath) is more difficult. This release needs to be gentle, and cannot involve an ejection charge, since such a charge would damage sensitive ATMOS measurements, as well as some of the CDLE's own control systems. In

order to gently deploy the CDLE in the proper orientation, we will use the CDLE Integration and Release Apparatus (CIARA).

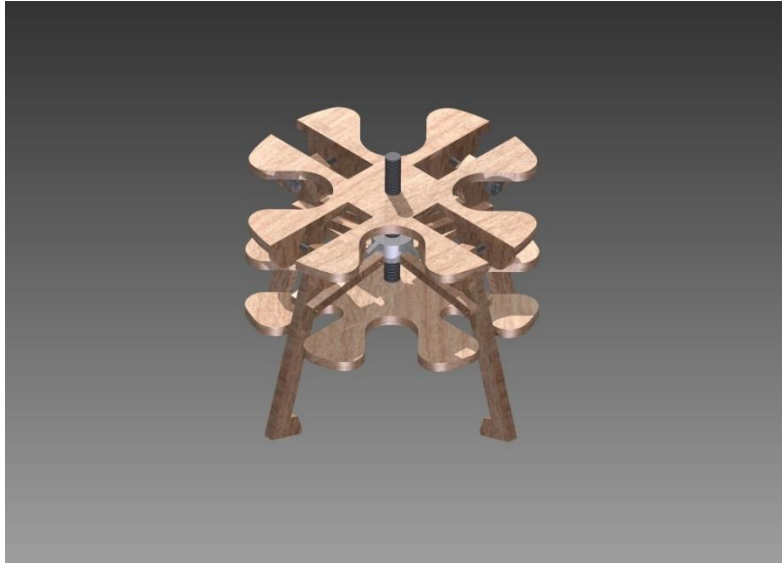


Figure 4.1.5.2 – CDLE release apparatus

The CIARA will consist of 4 latches that will be driven by a bearing that runs down a lead screw that will be driven by a motor and a gearbox, which have yet to be determined. This type of actuation enables a single linear movement to move all four latches at the same time. The bottom plate of the CIARA will have a strong spring on it. This spring will help push the quadcopter out once the latches are detached.

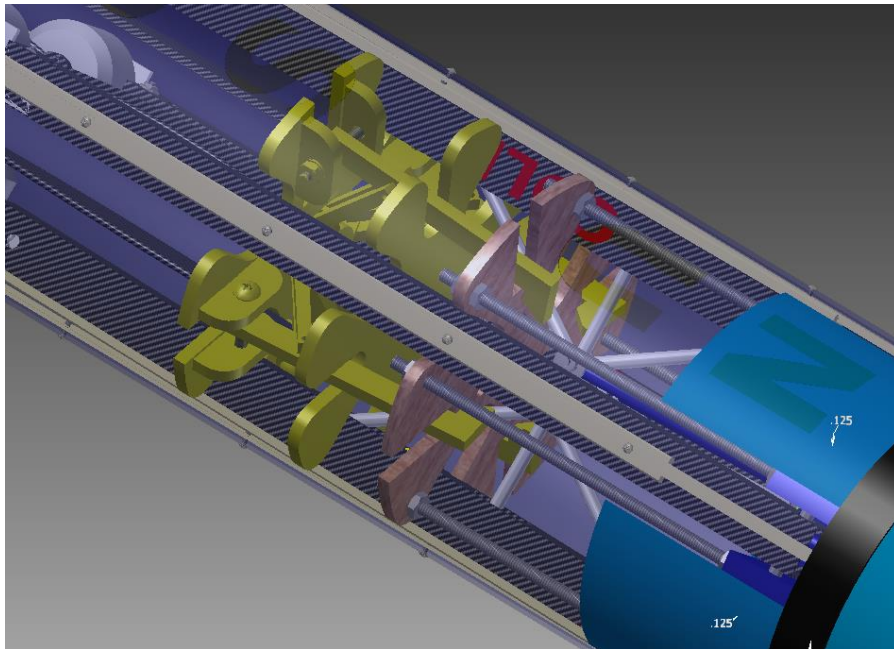


Figure 4.1.5.3 – CIARA interfacing with launch vehicle and CDLE

CIARA will interface with an interface plate that is mounted above the quadcopter with threaded rod. Once CIARA is engaged, the quadcopter will be securely locked in place until the latches are

released. As seen in the above figure, the CDLE is also attached with guide rails. These rails will ensure the deployment is as smooth as possible, and protect the CDLE during deployment as it would be undesirable for any damage to occur to CDLE due to the movement of the body tube.

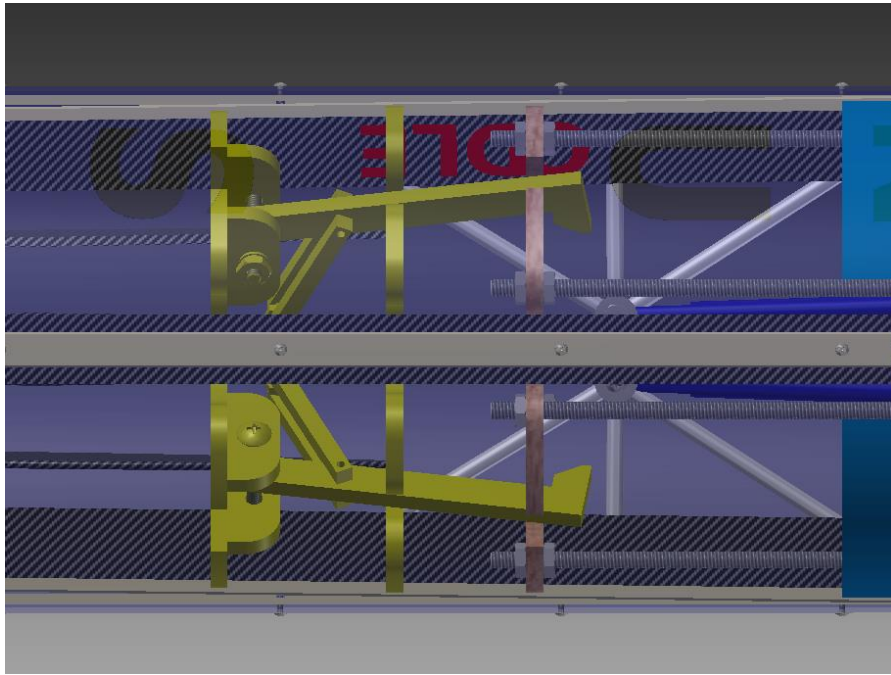


Figure 4.1.5.4 – CDLE mechanical latches

At apogee, when the motor turns on and CIARA's latches retract, the springs attached to the bottom plate of CIARA will push away the CDLE interface plate. This, combined with the deployment of the drogue parachutes out the back of the motor section, will be enough to ensure a safe and reliable deployment of CDLE.

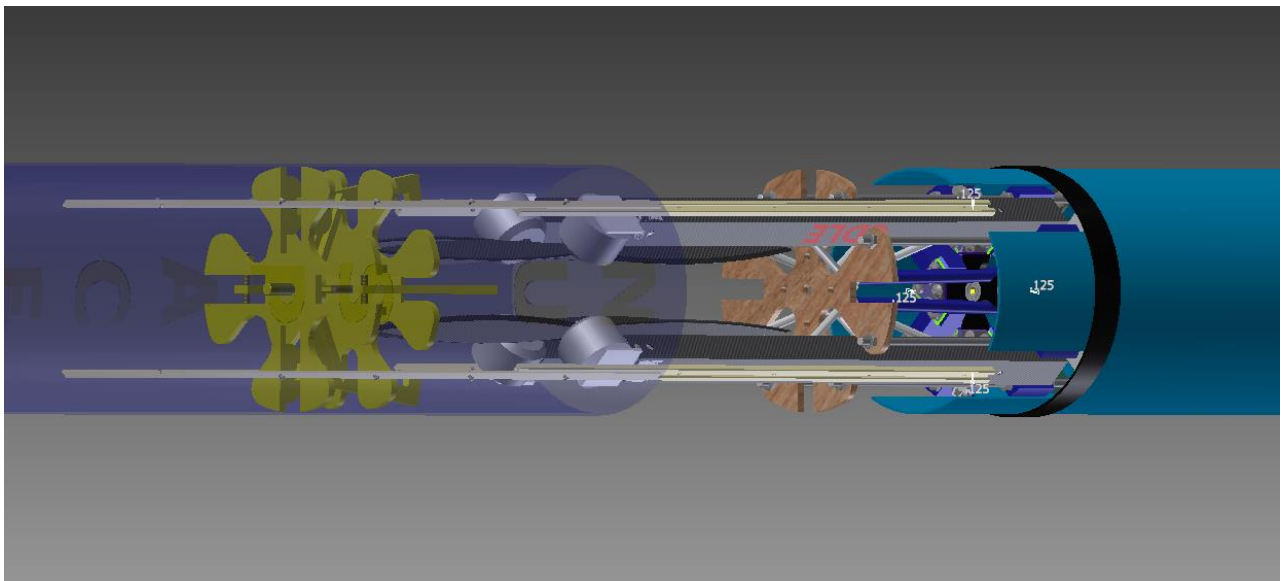


Figure 4.1.5.5 – CDLE interfacing with guide rails

The CDLE Sheath will then continue to travel with the motor section, and the CDLE will then start its arm deployment procedure.

4.1.6 Precision and Repeatability

The CDLE deployment and control systems will be capable of repeated, precise deployments utilizing the onboard software and hardware modules, as well as a controlled, repeatable deployment method.

The onboard software systems will be capable of utilizing accelerometer, gyroscopic, magnetometer, and telemetry data to determine the orientation of the quadcopter and to determine when the quadcopter comes into the correct orientation as it enters free fall. Once this orientation is confirmed by the on-board systems, the flight controller will trigger the deployment sequence, extending the arms until they are in their locked position, and armed.

Once these arms are fully extended, the CDLE will start up the motors and slow itself down from free fall to approximately 10 ft/s and utilize the GPS module onboard in order to determine its position within a 10ft spherical area. Once the quadcopter has decelerated and GPS position is confirmed, the quadcopter will alter its path and proceed to descend towards the landing coordinates provided for our landing area (34.891 N, -86.620 W). The CDLE will take a linear path towards this position as it descends until it arrives 10ft above the landing coordinates at a hover. At this point, the CDLE will hold position for 5-8 seconds before descending until it comes into contact with the ground, at which point, the motors will spin down, and the quadcopter will enter standby.

The combination of the on board accelerometers and the GPS data will be able to determine speed and acceleration within a reasonable margin of error. The CDLE will be able to stop within 50ft of our intended altitude.

The CDLE deploys in a fully repeatable manner, allowing for the possibility of rapidly re-deploying the landing system after a successful launch and landing. Upon landing, the CDLE enters standby, proceeds to transmit all collected data to ground command, and shuts down all motors. From this state, we will be able to recover the CDLE, recover the data backup from the ATMOS stored on the SD card attached to the subsystem, and remove the battery for recharging. Once the battery is charged, the CDLE can be reassembled and redeployed into another suitable rocket.

Reloading the CDLE for another launch will be done by simply replacing the battery in the quadcopter, and resetting the driving lead screw that controls the position of the arms, and loading the quadcopter into the body tube of the new launch vehicle. In the event of an abort, the CDLE will require that the parachute be repackaged and re-armed in order to allow for the possibility of another abort.

4.1.7 Drawings and Electrical Schematics

Below is the electrical schematic for the CDLE (Figure 4.1.7.1)

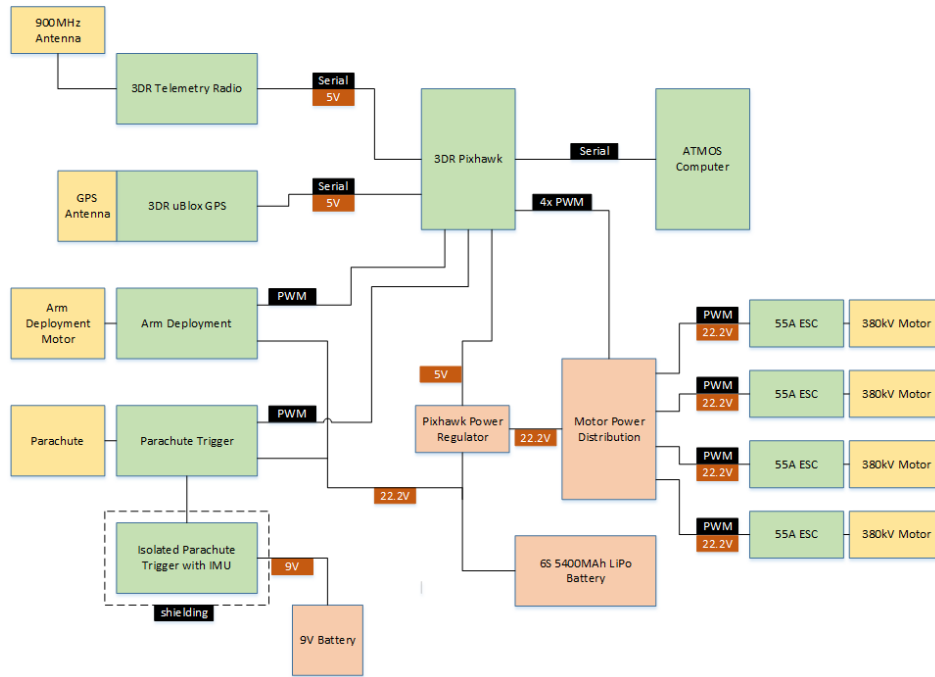


Figure 4.1.7.1 – CDLE electrical schematic

Below is the top view of the CDLE payload (Figure 4.1.7.2). Additional details of the CDLE payload can be found in 4.18 Key Components.

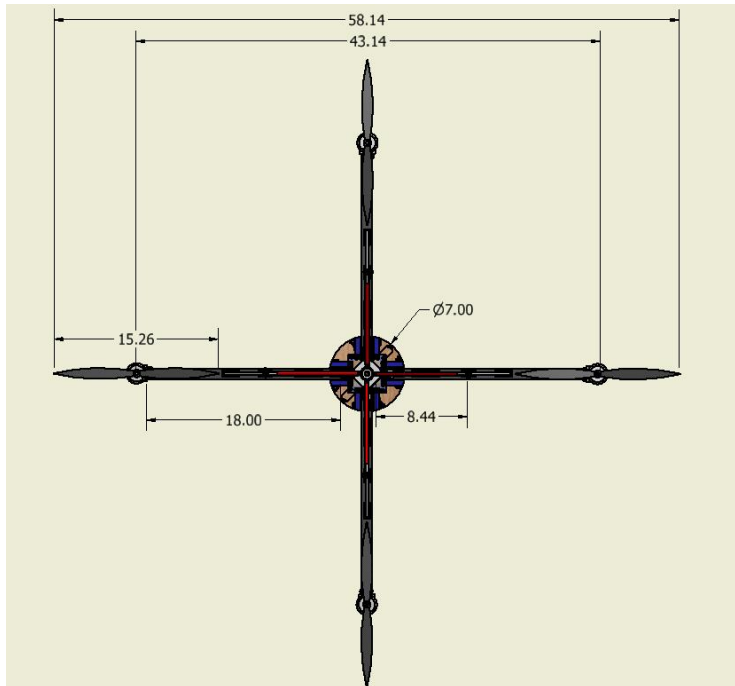


Figure 4.1.7.2 – CDLE top view

4.1.8 Key Components

The central component of the flight electronics is the 3DRobotics Pixhawk flight controller. This will control the entire descent process of CDLE, and ensure flight is stable for the ATMOS measurements. The Pixhawk has an accelerometer, gyro, magnetometer and barometer and uses an extended Kalman filter to generate accurate altitude, attitude, and heading estimates. In order to have accurate position data, the Pixhawk has a GPS receiver, sold by 3DR, connected over serial, and the GPS module also has a second magnetometer.

A 900MHz radio transceiver, also sold by 3DR, will provide a radio link to the ground station laptop. Another radio will be connected to a laptop to provide the other end of the radio link. Telemetry data will be sent from CDLE to the ground station, and the signal to trigger the parachute can be sent from the ground station to CDLE. There will also be a second radio and GPS system, broadcasting GPS coordinates in order to locate CDLE after landing, if necessary. In the event of a parachute deployment, the Pixhawk will send a signal through PWM to the trigger circuit, which will then fire the charge to deploy the parachute. To control each of the four propellers, the Pixhawk communicates with four electronic speed controllers (ESC) through four PWM channels. The ESCs take the PWM signal and generate an output to the motors driving the propellers. Finally, the Pixhawk will also drive the arm deployment motor through PWM to another motor controller.

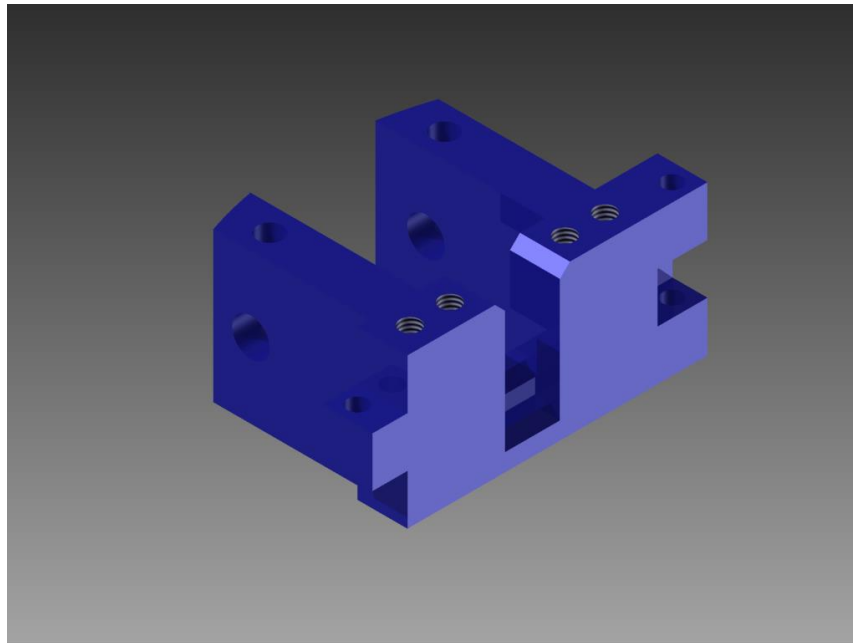


Figure 4.1.8.1 – CDLE chassis component

The main body of the chassis will be constructed out of identical sections (seen above in Figure 4.1.8.1). Each section will be machined out of Delrin plastic. In order to make sure each piece properly interfaces with its partner, each piece has a male and a female end. They will be secured together with an interference dowel. After they are securely lined up with this interference pin, the body will clamped together with screws to ensure it does not fall apart during flight operations.

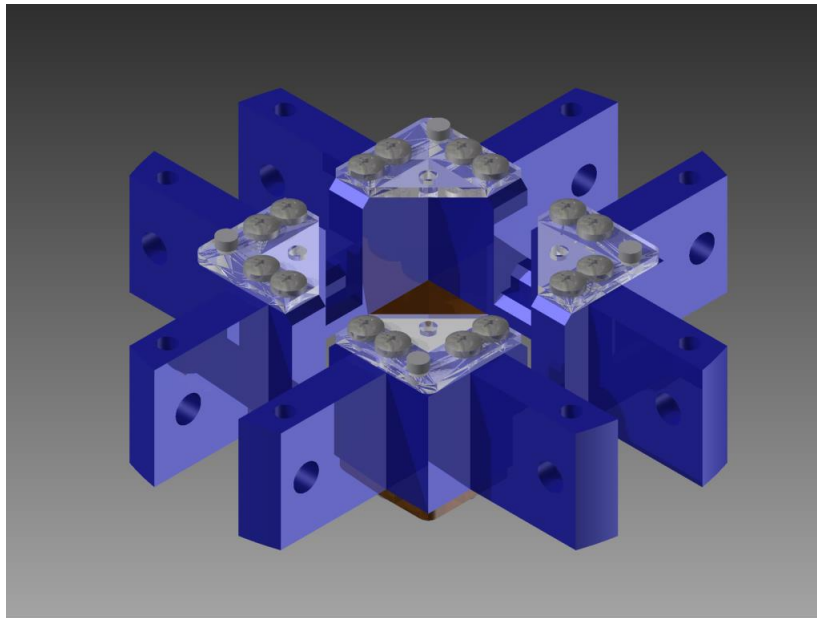


Figure 4.1.8.2 – CDLE chassis assembled

The body will be secured together with the interference pin and 10-24 screws that are attached to brackets which will be made of ¼ inch acrylic. There will be 8 brackets and 32 screws in total. This allows for maximum structural stability for the chassis of the quadcopter. The chassis also has 8 tapped holes on each side for ¼ -20 threaded rod in order to allow for us to attach the necessary structures to the quadcopter.

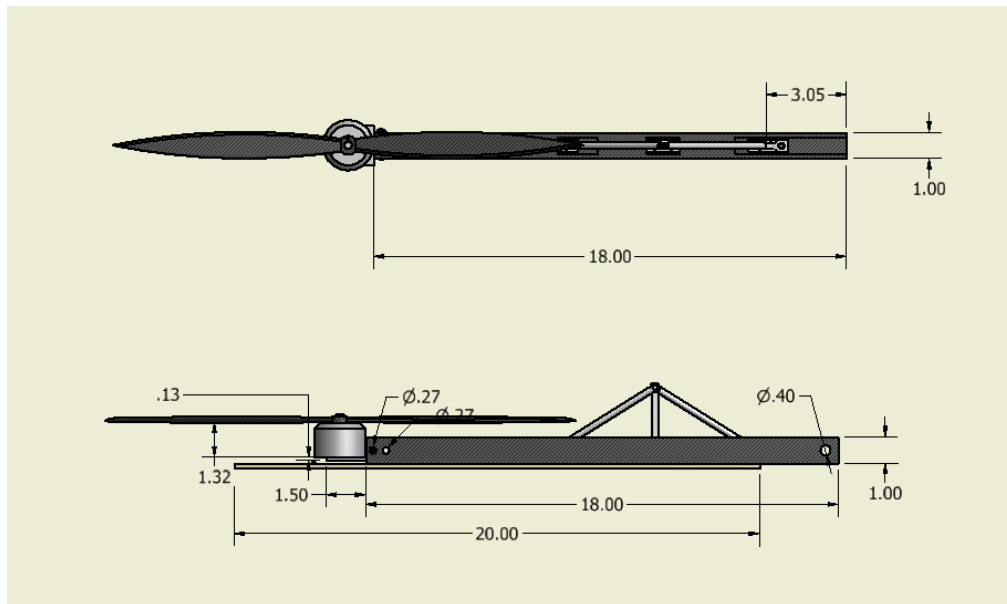


Figure 4.1.8.3 – CDLE arm

Each arm will be constructed by 1 inch by 1 inch carbon fiber square beams (see above in Figure 4.1.8.3). The square shape will provide a larger bending moment of inertia for the arm, and the hollow interior will allow wires to run out to the motors. Carbon fiber was chosen for its strength/weight ratio. The motors for the propellers will be mounted at the end of each arm. Each arm will be secured to the chassis with a pin, and latched in place with a mechanical lock to make sure they won't fold vertically mid-flight. On the top of each arm there will be a truss structure. This design will reinforce the strength in the arms for vertical forces (which will be the only significant forces acting on the arm, i.e. drag force and lift force from the propellers). This truss will provide additional support because it will be connected to the lead screw system which allows the arm to be deployed.

The arms will pivot around a 5/16 inch bolt. The bolt is 5/16 inch to increase resistance to bending, as bending the bolt that secures the arms to the pivot point would be less than ideal during flight.

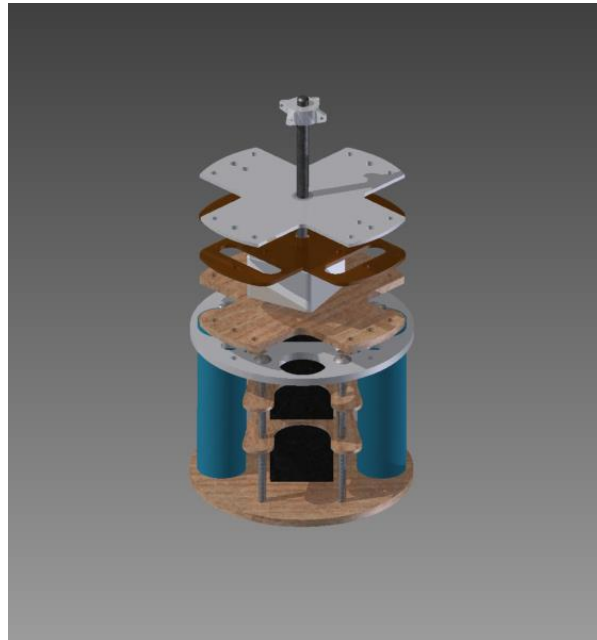


Figure 4.1.8.4 – CDLE lead screw

The lead screw drive contains some of the most essential components of the CDLE. The 5000mah battery, emergency parachutes, and flight electronics are all mounted in this one section. Also mounted here is a KDE1806XF-2350. This motor will power a gearbox which will drive the lead screw which will, in turn, actuate the arms. At 15 volts, the 2350 kV motor powers the gearbox to output a rotational velocity of 43200 RPM. The gearbox has a reduction ratio of 30:1, resulting in a final speed of 1440 RPM and a torque that is thirty times as powerful as the original input.

This section also holds the emergency parachute tubes. The emergency parachutes will deploy parachutes in the unlikely event of any flight anomaly. The emergency parachute tubes will be built out of a 38mm blue tube body tube and will have a bulkhead section set screwed into one end, allowing for easy access to the blast chamber. If the abort signal is sent, the black powder charge will pressurize the tube and the parachutes will shoot out, enabling the CDLE to land in a semi-controlled and safe manner.

4.2 Concept Features and Design - CDLE

4.2.1 Creativity and Originality

The CDLE system payload is a creative and original design that provides a difficult challenge, however yields a high reward. Featuring use of a deployable and reusable quadcopter, the CDLE system proves an innovative way to make complicated measurements, at a stable descent, that a normal launch vehicle would have difficulty producing. The measurements can also be taken for longer at exact altitudes due to the quadcopters ability to collect exact altitude data and compare it with other readings. The CDLE system also allows control of landing location. This feature opens the possibility of future launches over large bodies of water, with ability to land on a floating platform. This is a creative use of the system, allowing launches that most other payloads would be either destroyed in or unable to be recovered. In the unfortunate event of failure, the CDLE system features a safety mechanism that will bring the quadcopter down safely. The quadcopter is foldable and easily stored as a payload, allowing possible integration with different launch vehicles. Larger and more powerful launch vehicles enable the CDLE system to be possibly deployed at higher altitudes so that a larger amount of data can be collected. The CDLE system as a deployable and autonomous payload is an original design that demonstrates creativity while trying to accomplish otherwise challenging goals.

4.2.2 Uniqueness and Significance

The CDLE is unique as a rocket-deployed instrument platform because it provides a descent that is stable and controllable. Precise measurement of sky or ground data requires a stable instrument platform. Stable platforms ensure that measured data is collected under near identical conditions as time passes. Parachutes, while the standard for recovery of rocket payloads, do not provide a steady platform from which to make good measurements. The descent orientation of parachute-recovered payloads is unreliable and may result in sky measurements that are actually of the ground. The CDLE quadcopter provides a good platform from which to take atmospheric measurements by providing predictable orientation and position along all axes.

Having a controllable instrument platform allows the platform to choose a desirable sample on the ground. If a certain patch of ground is of interest to an on-board camera, being able to position the platform can ensure that the desired data can be collected. CDLE provides control over position and speed in all dimensions to provide maximal options for the instruments, although it does not currently scan the ground for points of interest.

Among quadcopters CDLE is unique because it is deployed from a rocket at apogee. While quadcopter frames exist that can fold, a frame that can unfold itself while falling is relatively unique, especially at the scale of CDLE. A limitation of traditional quadrotor design is that its flight time and payload is limited by its battery life. Rocket deployment extends the operable altitude and mission duration of drone-based instrument platforms. CDLE will reach 5280 feet in altitude before it needs to rely on its own motors. Operational altitude could be increased by using parachute recovery after relevant measurements have been made.

4.2.3 Challenge Assessment

Our design is suitably challenging. It involves launching a series of sensitive sensors on an autonomous drone out of our launch vehicle at an apogee of one mile. The CDLE must be ejected in a safe manner as to not damage any of its sensitive equipment. Then, it must autonomously fly to a predetermined set of coordinates while storing all of the sensor's constant readings onboard.

Meanwhile, if any part of this launch should go wrong, the launch vehicle is constantly waiting for a signal from a ground station connected to the rocket via MAV-Link protocol. If this signal from the ground station is received or something is detected to have gone wrong, the CDLE will automatically launch a parachute so it can land safely even in the event of drastic failure such as power failure. Finally, when the CDLE is near the ground, assuming there were no problems and the parachute was not needed to deploy, the CDLE still must land safely in a controlled manner, despite having just descended one mile. With all of this in mind, it is clear that our objective will be a suitable challenge for this project.

4.3 Science Value - CDLE

4.3.1 Objectives

The goal of the CDLE payload is to provide a good platform for the ATMOS instruments. To this end, CDLE should eject safely from the launch vehicle, gain control quickly, and provide a safe and controlled descent to the ground.

4.3.2 Success Criteria

In accordance with the objectives, the CDLE payload will be considered successful if the quadcopter:

- Is deployed when the rocket separates at apogee.
- Opens its arms, powers its motors, and stabilizes itself autonomously after deployment.
- Autonomously lands at the target location.
- Is not damaged during descent or landing
- Does not require the use of the safety parachute or manual control.
- Successfully relays all relevant data captured during and after flight

4.3.3 Logic and Approach

We theorized that we could control the descent of a payload from a launch vehicle. Possible applications for this would be more accurate landing of crucial payload within a target area, or multiple landings of crucial payloads in multiple target zones.

We determined that the best way to do this would be in the form of a quadcopter inside the launch vehicle. We chose a quadcopter because of its versatility when it came to diversified tasks. Also, using a quadcopter integrated with ATMOS, atmospheric readings can be taken from multiple locations. Finally, a controlled payload could return to its origin site, and deposit readings, as well as other precious cargo it may have picked up.

While planning the mechanical design of the quadcopter CDLE, we determined the following important design features as required by this task:

1. Must be able to fit in the launch vehicle
2. Must be able to be deployed from a launch vehicle
3. Must be recoverable and reusable

First, we considered the first feature required. Because a quadcopters generally have a wide arm-span that would not fit in the cylinder of the launch vehicle, we designed the arms of CDLE to pivot upwards, decreasing the arm-span to that of the diameter of the launch vehicle. During deployment, the arms will pivot downwards, where a separate locking mechanism will secure them in place. Simply orientating the propellers along the arms while being inserted into the launch vehicle will enable the propellers to fit without problem. Also, quadcopters generally have its electronics on the central plate that adjoins the arms. However, because the arms will be pivoting, this space no longer available. Instead, a cylindrical compartment will be attached to the underside of the center of the arms, which will house all electronics as well as mechanical components to lower the arms and a parachute in the event of failure.

To address the second requirement, metal clamps were installed inside the launch vehicle to secure CDLE during launch and ascent. Inside the launch vehicle, a spring will be installed and position under the electronics compartment, that will push CDLE out of the launch vehicle during deployment at apogee. Inside the launch vehicle, there will also be guide rails. On the arms of CDLE, we will install guide buttons, to control how CDLE unveils when ejected from the launch vehicle.

Considering the third requirement, we plan to use high strength materials in all parts of the CDLE, which will be able to withstand impact in the event of catastrophic failure and uncontrolled descent. Also, all mechanical locks will be able to be manually unlocked.

4.3.4 Testing and Variables

The CDLE's individual components will be tested in a controlled environment, including the arm folding mechanism, the arm locking mechanism, and the guide rail system within the launch vehicle, to determine each system's success repeatability and dependability. We will also do strength tests on materials to determine the amount of impact the CDLE can withstand in the event of failure, or repeated stress. We will do full system tests that will execute the entire deployment sequence of the CDLE in a controlled setting. These should simulate the post-deployment chaos, and give us a basic understanding of how long the CDLE requires to stabilize itself. In a similar fashion, we will also test the emergency failure sequence, where all electronics are immediately turned off and an emergency parachute is deployed.

4.3.5 Relevance of Data

The data from these tests will provide a basic understanding of how much stress the CDLE can withstand and how dependable the mechanical systems are. Because the CDLE will be tested in a controlled setting which will not account for certain factors in a realistic setting,

such as wind and post-deployment chaos, a factor of safety will be added to all variables and measurements to ensure success in any high stress situation.

Deviations from the expected flight track and vehicle condition either indicate design problems or invalid assumptions when making predictions. After flight, any data that differs from expectation will be analyzed. Solutions will be proposed if design problems are indicated by the data.

4.3.6 Preliminary Experiment Process

There is a multitude of experiments that will benefit the design of the CDLE system. Examples of these experiments are listed in Table-4.3.6:

Table 4.3.6 – Preliminary experiment process for the CDLE

| Experiment | Objective |
|--|---|
| Stress test of quadcopter arm materials | Determine the amount of stress at which the quadcopter arms fail in order to make an educated decision on arm material. |
| Thrust test of different combinations of motors, propellers, and batteries of the quadcopter | Determine the thrust generated by the motors and propellers with different batteries, to determine the lightest component options while still producing ample thrust. This data will also contribute to the quadcopter’s maximum flight time. |
| Arm deployment test | Determine the reliability of the design of CDLE’s foldable arms. Check that it can take the load of deployment successfully with a high rate of repeatability. |
| Crash test | Determine a safe ground impact velocity for the CDLE system, for both normal flight and in and abort / failure case. |
| Flight simulation | Determine that all software components operate and communicate, and that the flight plan is followed. Also verify all fail safes implemented in software. |
| Flight tests | Determine if the quadcopter is able to maintain safe flight autonomously. There will be multiple experiments to test if the quadcopter is able to complete the following objectives: <ul style="list-style-type: none"> a. Basic flight b. Controlled Landing c. Ability to land at specified location d. Ability to regain control in momentary chaotic situations |
| CDLE deployment test | Determine if the CDLE system is able to be deployed from the launch vehicle and which conditions required to do so. |

4.4 Selection, Design, and Verification – ATMOS

4.4.1 System Review

In order to create a payload for taking atmospheric measurements, we created the ATMOS: Atmospheric and Topographical Measurements Optics Suite. The ATMOS will measure, record, and transmit data on temperature, pressure, altitude, relative humidity, solar irradiance, and ultraviolet radiation. It will also collect images of the horizon in the visible spectrum and of the ground in the infrared (IR) spectrum. The ATMOS is comprised of two main data collecting systems: an Arduino Uno and a Raspberry Pi. All numerical atmospheric data collected by the ATMOS is under the domain of the Arduino Uno while any image processing (both visible and infrared) is handled by the Raspberry Pi. Any and all data or images will be stored on SD card on-board the ATMOS, and will be transmitted upon landing. We chose these systems because each is adept in their respective areas of use; it is favorable to have a microcontroller managing the analog sensors while a microprocessor handles the more complex image processing. The ATMOS is designed specifically to fit the harsher design constraints that come from being held in the CDLE, which is itself ejected from a rocket in flight.

4.4.2 Subsystem Descriptions

The Arduino Uno is in control of a BME280 Atmospheric sensor, a ML8511 UV sensor, a solar irradiance sensor, an SD card module, and an RF transmitter. Two Raspberry Pi camera modules, a Pi NoIR, and a Lepton FLIR are all controlled by the Raspberry Pi. The two systems will communicate using analog voltage pulses to initiate measurement readings in one or the other. The program being run on the Arduino will use the pressure reading to infer the altitude.

The BME280 atmospheric sensor will detect temperature, pressure, and relative humidity. The ML8511 UV sensor will detect ultraviolet radiation. The solar irradiance sensor will measure solar power output via a photodiode system of our making. The SD card module will store information on board, and the RF transmitter will transmit the atmospheric data back to ground after landing. The visible light camera will take pictures of the horizon during descent, and the IR cameras will take pictures of the ground for analysis of vegetation density and atmospheric transmittance. These will be kept and stored on the Raspberry Pi to be transmitted to the ground station after landing.

Table 4.4.2 – Operating system, ATMOS sensor, and corresponding mission

| System | Sensor (Subsystem) | Mission |
|---------|--------------------|------------------|
| Arduino | BME280 | Pressure |
| Arduino | BME280 | Humidity |
| Arduino | BME280 | Temperature |
| Arduino | Photodiode system | Solar Irradiance |

| | | |
|--------------|----------------------------|---|
| Arduino | ML8511 | UV Radiation |
| Raspberry Pi | Raspberry Pi Camera Module | Visible Spectrum Imaging |
| Raspberry Pi | Pi NoIR | NDVI |
| Raspberry Pi | Lepton FLIR | Surface Temperature and atmospheric transmittance |

4.4.3 Performance Characteristics

After the ATMOS payload is separated from the launch vehicle at apogee, it will descend, taking atmospheric measurements once per second (1Hz). In addition to atmospheric data, images will be taken 5 times each in the visible and infrared spectra. When the payload has landed, 3 more visible spectrum images will be taken and atmospheric data collection will slow down to be measured once per minute (16mHz). Ten minutes after landing, data collection will cease. During this process, all data will be stored on the ATMOS using an SD card. The numeric atmospheric data will be transmitted to our ground station using RF transceivers.

Afterwards, we will check our atmospheric data by using known data for given altitudes. We will also look for expected correlations such as a net increase in pressure and a net decrease in solar irradiance during the descent.

4.4.4 Verification Plan

We have successfully wired the BME 280, UV Sensor, and data logger to the Arduino. All the data that has been collected in certain preliminary tests has been very similar to accepted values obtained from other measuring devices. The data is successfully stored on the SD card. The next task will be to wire the photodiode and analyze the data. We will then wire all the camera systems to the Raspberry Pi and work with the CDLE software team to transmit the data wirelessly.

Figure 4.1.8.1 – ATMOS verification plan

| Payload Requirement | Design Feature | Verification |
|---|--|--|
| Pressure readings taken every ten seconds during descent and then once every minute after landing | Adafruit BME 280 sensor, wired to Arduino with a real time clock | Analysis – Pressure readings will be compared to accepted pressure vs altitude data Test - sensor will be tested on the ground to verify that measurements are taken at the proper time increments. |

| | | |
|---|--|---|
| Temperature Readings taken every ten seconds during descent and then once every minute after landing | Adafruit BME 280 sensor, wired to Arduino with a real time clock | Test- Put sensors in areas of known temperature and then compare the data to the accepted values. |
| Humidity Readings taken every ten seconds during descent and then once every minute after landing | Adafruit BME 280 sensor, wired to Arduino with a real time clock | Test- change humidity of environment and see if measurements change accordingly |
| Solar Irradiance Readings taken every ten seconds during descent and then once every minute after landing | Photodiode wired to Arduino, taking output voltage readings from the analog pin. | Test- change the exposure to the sun and see if measurements changes accordingly. Also, compare readings to that of a pyranometer to quantify the accuracy. |
| Ultraviolet Radiation (UV) Readings taken every ten seconds during descent and then once every minute after landing | ML 8511 UV Sensor wired to Arduino | Test- change the exposure to the sun and see if measurements changes accordingly. |
| At least two pictures during descent and three after landing. | Raspberry Pi camera module | Inspection- See if we get adequate images at appropriate times during test flight |
| All pictures must be of the horizon with the sky in the top of the frame and the ground in the bottom | Quadcopter software to ensure stability | Visual Inspection of photos taken during test flight |
| Store Data onboard | SD Card wired to Arduino and Raspberry Pi | Inspection- verify data is on SD card |
| Transmit Data | Data will relayed through flight controller to radio antenna | Inspection- Successful if data is received |
| Vegetation Analysis | Pi NoIR Camera Module and visible light camera | Analysis- receive images and compare visible light to IR light to place on NDVI scale |
| Atmospheric Transmittance Data | Lepton FLIR | Inspection – receive images and analyze images to get reputable data |

4.4.5 Preliminary Integration Plan

CDLE will be designing their quadcopter system knowing the approximate weight, sizes, and necessary orientations of each sensor. ATMOS will feed the CDLE group more precise information regarding the sensors and the wiring as each system is prototyped. To transmit the data, we will be working with the CDLE software team who will already be using a radio in their system. ATMOS will be sending data to the Pixhawk flight controller, which will then transmit the data over the radio.

To test if they are working properly in an actual flight, a few of the ATMOS components will be integrated into the subscale rocket. The BME280, which will be gathering pressure, temperature, and humidity data, as well as the Raspberry Pi Camera Module, which will be taking pictures of the horizon, will be tested in the subscale rocket. This will allow us to test the BME280 to verify the data. We will also be able to test the clarity of the pictures taken while falling at a given speed. This will give us an estimate of the maximum speed that the quadcopter can descend at that will still allow for useful images to be taken.

To test their software, the CDLE software team will be building a test bed quadcopter. We will use this quadcopter to test all of the ATMOS components that require exposure to light. This includes the photodiode to measure solar irradiance, the UV sensor, and all of the necessary cameras (Visible light, Pi NoIR, and Lepton FLIR). The solar irradiance data will need to be corrected considerably. We believe that the photodiode will reach its maximum voltage output quickly when exposed to direct sunlight. We plan to attenuate the incoming sunlight with filters so that the diode will not saturate immediately and any changes in output voltage can still be observed. The change in voltage will then be corrected to read proper solar irradiance data. The solar irradiance measurements, as well as all cameras, will require a certain amount of stability to get good data. By testing all of these components on the test bed of the quadcopter, we will be able to communicate to the software team whether or not their current configuration is stable enough for accurate readings. We will also get sample IR images from this flight, from which we can begin analysis to develop a system for gathering quantifiable data from them. When it comes time for the flight in Alabama we will be able to quickly make conclusions from all the data and images about the surroundings.

4.4.6 Precision and Repeatability

Below is a table showing degree of precision we can record for each sensor:

Figure 4.4.6 – Sensor precision

| Sensor | Degree of Precision |
|----------------------|-----------------------------------|
| BME 280 | .1 |
| UV Sensor | .1 |
| Solar Irradiance | 1 |
| Visible light camera | Native Resolution of 5 megapixels |

| | |
|-------------|-----------------------|
| Pi NoIR | 5 megapixels |
| Lepton FLIR | 80 x 60 active pixels |

It should be noted that solar irradiance could be measured to more decimal places because the output voltage can be measured more precisely. However, since there are many factors that affect that accuracy of this measurement, such as angle of the sun in relation to the sensor, we have decided to only measure integer numbers.

There are a few matters of concern regarding the repeatability of some of the measurements. Because the measurements are being taken on the quadcopter, the propellers will disturb the surrounding air. We plan to enclose the BME280 to minimize those effects, but we will be sure to compare the data with the data from the subscale flight where the surrounding air is unaffected by propellers. This will give us some insight into the effects of the quadcopter's disturbed air on our measurements.

The stability and orientation of our quadcopter could affect the repeatability of the measurements requiring light. The quadcopter will not be able to maintain the same stability throughout flight as it must move to reach a particular destination and will be affected by wind and other atmospheric factors. The solar irradiance data relies heavily on the orientation of the sun with respect to the photodiode. This means time of day as well as stability will have to be considered when taking these readings. The camera clarity for our IR images is also dependent on the stability of the quadcopter. We will be working with CDLE to ensure we can reach the stability needed to gather images that can be analyzed.

4.4.7 Drawings and Electrical Schematics

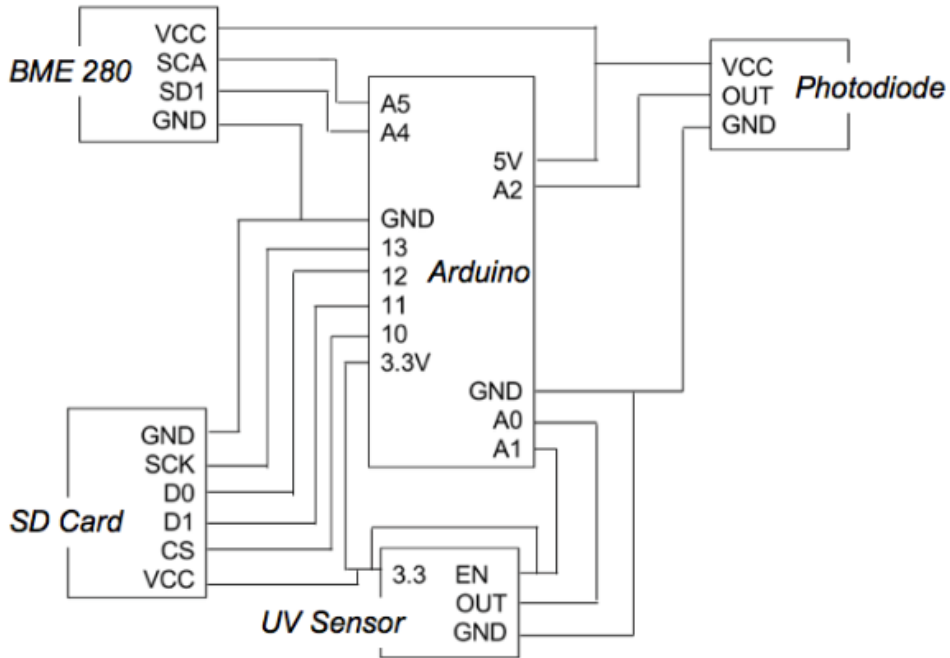


Figure 4.4.7.1 – ATMOS electrical schematics

The electrical schematic above shows the wiring for the Arduino. The BME280, the UV Sensor, the photodiode to measure solar irradiance, as well as the SD card, which will be storing all of our data, are all wired to the Arduino, leaving the cameras to run off of the Raspberry Pi. Our prototype wiring for the BME280, UV sensor, and SD card can be seen in the photograph below.

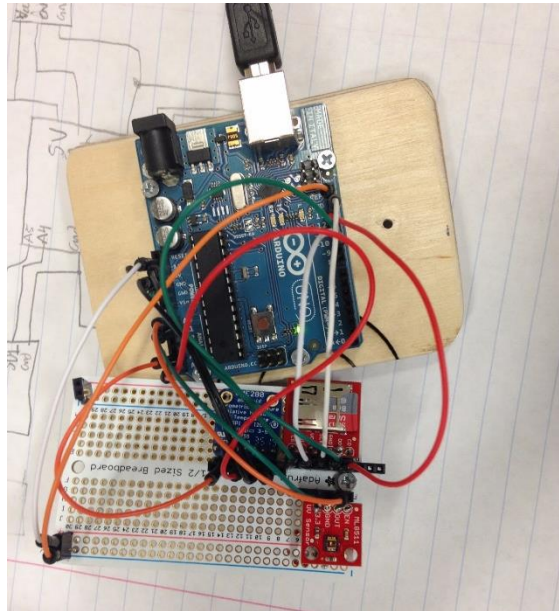


Figure 4.4.7.2 – ATMOS wiring prototype

4.4.8 Key Components

There are several key components to the ATMOS payload. In order to accomplish the mission objective, which is to collect data for studying the atmosphere during descent and after landing, including measurements of pressure, temperature, relative humidity, solar irradiance and ultraviolet radiation, there will be a total of seven components wired to either the Arduino Uno or the Raspberry Pi. Firstly, upon descent, the BME280 will gather measurements for temperature, pressure, and humidity. Simultaneously, the ML8511 UV sensor and photodiode will collect high-altitude ultraviolet radiation and solar irradiance data, respectively. In addition, there will be a Pi NoIR camera, Lepton FLIR camera, and visible light camera which are the central components to determine the atmospheric transmittance and plant density through NDVI. These components will work in conjunction with an SD card and data logger module and RF Transmitter which will log all the collected readings on-board the quadcopter in a micro SD card and wirelessly transmit the data to the ground station.

4.5 Concept Features and Design – ATMOS

4.5.1 Creativity and Originality

The ATMOS design will feature an array of creative and original features. Most notably, we will have the sensor suite mounted to a quadcopter payload, the CDLE, which will enable an actively controlled descent. While the quadcopter makes a controlled descent, the ATMOS will collect and store data on board. This data will include measurements from a unique method of determining solar irradiance, an original design to determine the atmospheric transmittance of the atmosphere, and an innovative process to differentiate plant matter on the ground located below the CDLE. To determine the solar irradiance the ATMOS will feature a subsystem containing a photodiode. This photodiode will generate current proportional to the intensity of light that it detects. The generated voltage will be measured with a digital potentiometer and. This solution was proposed in place of using a pyranometer to remain within the size and weight constraints of the design. In addition to the required NASA SL 2016 measurements, the ATMOS will feature two original experimental measurements. First, there will be an original design to determine transmittance of the atmosphere. This will be accomplished with a Lepton FLIR camera on the bottom of the quadcopter which will measure intensity through the collection of images in the long wave infrared spectrum -- wavelengths from 8 to 14 microns. The ATMOS will record the intensity as a function of altitude upon descent. Second, this design will have a visible light camera as well as a Raspberry Pi NoIR camera mounted to the base of the quadcopter and facing downwards. This camera will take images in the near end of the infrared spectrum. The visible light images will be compared to the near end infrared images and work in conjunction with the Normalized Difference Vegetation Index (NDVI) to calculate plant density. These experiments rely heavily on data originated from images as well as an optimal solar zenith angle with regard to the photodiode and UV sensor. By integrating the ATMOS with a quadcopter, AIAA at NU will collect quality pictures of a known orientation and will maximize stability. This will therefore facilitate an atmospheric measurements payload that will have the most accurate data possible.

4.5.2 Uniqueness and Significance

There is a great deal of significance in determining atmospheric characteristics using a lightweight, compact, cost-efficient, and versatile Atmospheric and Topographic Measurements Optics Suite. By employing the Bosch BME280 environmental sensor, ML8511 UV, solar irradiance sensor, an SD card module, an RF transmitter, and Pi NoIR cameras, the ATMOS will successfully determine all required atmospheric measurements while remaining well within the mass constraint created by the quadcopter lift limit. This sensor suite is projected to be a maximum of one kilogram which demonstrates the lightweight suitability to an assortment of aerial vehicles. A notable feature of the system is that the entire ATMOS will also be relatively compact. The BME280, ML8511, SI sensor, and UV sensor will all be mounted to a single breadboard. This compacted design will enable this payload to be easily integrated into the framework of the CDLE. The ATMOS will have a broad range of significant scientific applications, ranging from high-altitude temperature data collection to autonomously identifying the variance between the topographical features, specifically plant matter, below the quadcopter. With the calculation of plant density, it will be possible to determine if the vegetation is abundant and healthy. In addition to these measurements, the data collected will be wirelessly transmitted to a receiver at home base via an RF transmitter. This will enable our data to be analyzed by the ground team to either confirm or refute the hypothesized results.

4.5.3 Challenge Assessment

One crucial challenge that the ATMOS will face is the integration with the CDLE payload. While the CDLE has unique benefits, due to the constraints on the CDLE lift as well as the physical dimensions, the ATMOS must remain within a specified weight and size. In addition, since the Lepton FLIR, visible light, and Pi NoIR cameras must permanently face the ground and the horizon, the location of the sensor suite on the quadcopter will be integral to the success of accurate data collection. It will also be important that the sensor suite be isolated from the pressure differences created by the quadcopter propellers to obtain accurate pressure readings. These design requirements have been taken into consideration and the current layout of the ATMOS and the CDLE integration can be seen in Figure 4.5.3.1.

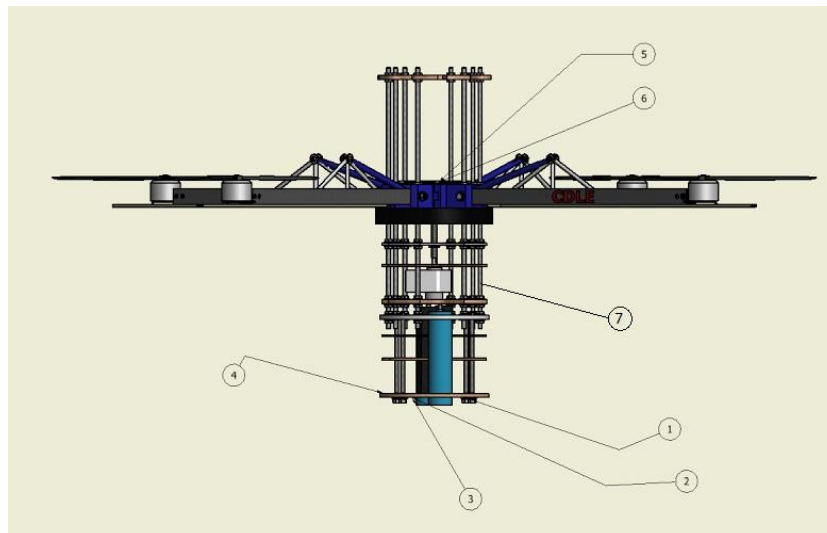


Figure 4.5.3.1 – Projected ATMOS placement on CDLE. Refer to Figure 4.5.3.1 for component key

Table 4.5.3.1 – Component key for ATMOS placement on CDLE

| Number on Figure 4.5.3.1 | ATMOS Component with Required Orientation and Placement |
|--------------------------|---|
| 1 | Pi NoIR |
| 2 | Lepton FLIR |
| 3 | Raspberry Pi Camera Module |
| 4 | Raspberry Pi Camera Module |
| 5 | M8511 UV Sensor |
| 6 | Photodiode |
| 7 | BME280 |

4.6 Science Value – ATMOS

4.6.1 Objectives

There are numerous applications of a self-contained and autonomous sensory drone. Some potential uses include survey in the fields of agriculture, meteorology, military/defense, aerospace, and research. The ATMOS payload gains its versatility from its suite of sensors. The drone system is capable of measuring air temperature, humidity, pressure, solar irradiance, UV radiation, surface IR radiation, and atmospheric transmittance. This broad range of data is useful in many fields. ATMOS can assess crop health for agricultural applications, examine weather patterns to help predict storms, and determine incident irradiance for the solar energy industry. The objective of the ATMOS payload is to verify that small, inexpensive drones can be used to consistently and accurately take measurements for these applications. Therefore, the ATMOS is intended to be a robust atmospheric measurement sensing system that is able to take measurements and photograph its surroundings in the visible spectrum and photograph the surface in the infrared spectrum.

4.6.2 Success Criteria

The ATMOS payload will be said to succeed in the case that all of its subsystems function successfully to collect data at the correct times and transmit the data to the home base after landing. Its sensors must take measurements of the atmospheric temperature, pressure, relative humidity, incident solar irradiance, atmospheric transmittance and UV radiation every second between drone deployment and landing. These measurements must be accurate within a certain range. These value are compared to the accepted values or values obtained from ground-based sensors that are verified as accurate. Table 4.6.2.1 (on the next page) lists accuracy for each.

Table 4.6.2.1 – ATMOS sensor accuracy

| Measurement | Accuracy |
|---|---------------------------------|
| Pressure (Pa) | $\pm 0.25\%$ |
| Temperature ($^{\circ}\text{C}$) | $\pm 1\text{ }^{\circ}\text{C}$ |
| Relative Humidity (%) | $\pm 3\%$ |
| Solar Irradiance (W/M^2) | $\pm 5\%$ |
| UV Radiation | $\pm 1\%$ |

The ATMOS also has multiple cameras. One camera will take pictures of the surroundings from multiple altitudes. Another will take pictures of the ground in the near IR spectrum, and a third will take pictures of the surface in the long wave IR spectrum (thermal imaging). The success criteria for these systems include taking the picture at the correct altitudes with sufficient clarity so that features such as the horizon and sky can be distinguished. For the IR cameras, the system will be successful if multiple regions of varying IR wavelengths and intensities can be discerned. This would allow for different surface features and topography types such as vegetation, human structures, and surface water to be distinguished. However, this data processing is not done on board and is not considered in the evaluation of our payload.

Finally, the radio communications systems are considered successful if the data is transferred quickly and completely to the home base after landing.

4.6.3 Experimental Approach and Rationale

4.6.3.1 Analog Sensors

The atmosphere's temperature, relative humidity, and pressure as well as the solar irradiance and UV radiation change depending on one's location and altitude. This is due to global weather patterns and the structure of the atmosphere. It is presumed that for low altitudes the temperature and pressure decrease linearly with rising altitude and that the latitude of the location will only scale the measurements by a small factor. If this is the case, a global model for the temperature and pressure of the low atmosphere can be created. This model negates the effects of large land features such

as mountain ranges. Humidity, on the other hand, is a highly variable condition of the atmosphere that depends on location and time of year. It is also presumed that the UV radiation and solar irradiance will not change very much with rising atmosphere, but may change slightly with location and will change with latitude due to the angle of the sun. Our experiment will measure these values and we will be able to use the data obtained to create models. If the ATMOS payload were to fly on multiple missions at different points throughout the year, more patterns may emerge.

The ATMOS will collect atmospheric data using 3 sensor subsystems. These are connected to the analog pins of an Arduino board which will log the data on a micro SD card. The first sensor is an Adafruit BME280 which measures temperature, humidity and pressure. The second is an ML8511 from SparkFun which measures the UV intensity using a photodiode. The third is a photodiode sensitive to a wide range of wavelengths in the visible spectrum for the solar irradiance measurement.

4.6.3.2 Visible Imaging

Imaging will be done by camera modules on board the quadcopter. One horizontal Raspberry Pi, one downward facing Raspberry Pi, one downward facing Pi NoIR (No IR filter) module, and one Lepton FLIR for longwave IR.

4.6.3.3 NDVI

The ATMOS will be mapping the topography of the surface by using a method known as Normalized Difference Vegetation Index (NDVI). NDVI is used as a way to determine the density of live green vegetation in a given area. It has been used by instruments on NASA satellites to measure the amount vegetation in different areas of earth. The NDVI at a given pixel is given by:

$$NDVI = \frac{(NIR - VIS)}{(NIR + VIS)}$$

4.6.3.4 Atmospheric Transmittance and Thermal Imaging

The makeup of the atmosphere is critical to the health of our planet. One way to investigate the makeup of the atmosphere is to measure the amount of light it absorbs. This is called the transmittance. Knowing this value can help determine the concentrations of certain gases such as water vapor, nitrogen, methane, and carbon dioxide. Transmittance is defined as the ratio of the transmitted radiant flux to the incident radiant flux. In other words, the percentage of light that is transmitted through a material.

$$T = \frac{\varphi_t}{\varphi_i}$$

The transmittance of a material depends on two factors, the length of the path the light takes, and the attenuation coefficient, also known as the absorption coefficient for gases, of a material. This gives rise to the Beer-Lambert Law:

$$T = e^{-kx}$$

Where k is the absorption coefficient of the low atmosphere and x is the path length that the light goes through. It is a decaying function; as the distance the light travels grows, there is less and less of it that survives the trip. By measuring the intensity of the light at multiple distances and knowing the intensity of the light at $x = 0$, it is possible to calculate the k for the atmosphere.

This will be done using a downward facing, long wave IR camera. This camera was chosen because very little sunlight is emitted in the long wave IR spectrum, so the only IR light measured will be from the ground. The ATMOS will measure the light in the IR spectrum at multiple altitudes while descending, and measure a value for “incident” light at a certain low altitude, A_0 (~ 100 m). The transmittance of the atmosphere between A_0 and A will be the intensity reading obtained by the camera, $I(A)$, divided by the incident light, $I(A_0)$. If the transmittance $T(A)$ is plotted with respect to A , we should obtain an exponential relationship, which can be rearranged to a linear relationship in which we can measure the absorption coefficient:

$$T(A) = e^{-kx}$$
$$K = - \frac{\ln(T(A))}{A}$$

The last equation is equal to the slope of the plot of the natural log of the transmittance with respect to the altitude.

The intensity of the IR light that the camera measures will not just be used for atmospheric transmittance measurements. It will be also used for surface topography. The images obtained by the camera are representative of the temperature of the surface. This is due to the phenomenon of black body radiation. The amount of light of a certain long wave IR wavelength increases to a maximum as the temperature of the black body rises. Only when an object is very hot does it emit near IR or even visible light. Consider the coals that glow red or orange as they heat up. This is why LWIR is used for thermal imaging. The camera will conduct thermal imaging of the surface, which will allow us to identify different features with stark contrasts in temperature such as surface water, which has a relatively low temperature, soil or vegetation.

4.6.4 Preliminary Experiment Process

We will be testing each experiment individually through several simulations before we launch the ATMOS. For the atmospheric and solar sensors, we will run physical simulations through a wide range of data points looking to individually calibrate each sensor consistently and accurately. We will also test data timing and collection accuracy via software simulations to ensure that the ATMOS is aware of how and when to take measurements. The utmost caution will be taken in performing all experiments, especially those that involve extreme

temperatures, UV radiation, or CDLE.

4.6.4.1 Analog Sensors

For many of the physical tests, we will be flying the ATMOS on a testbed quadcopter collecting data on temperature, humidity, and pressure during the whole of the ascent and the descent. Mapping the data and its given altitude will allow us to make note of any discrepancies with expected data, and we will make calibrations accordingly. We will also test the sensor by placing it in various controlled environments and varying temperature, humidity and pressure and monitoring the sensor response.

4.6.4.2 Visible Imaging

Like the previous tests, when we fly the ATMOS on the testbed we will also take images using the various camera systems. We want to ensure that the visible spectrum images contain both the ground and the sky. In addition to simple ground tests, we will analyze the effective use of the infrared cameras when aimed at the ground from the air.

4.6.4.3 NVDI

According to many hobbyists, it is possible to use NDVI to identify vegetation even at low altitudes -- although the results are not very groundbreaking; it is easy to identify trees and grass from altitudes of 100 feet. A preliminary test of the Pi NoIR camera will be to use NDVI to increase the contrast between live green vegetation and other terrain.

4.6.4.4 Atmospheric Transmittance and Thermal Imaging

The preliminary experiment process for the LWIR camera will include measuring light intensity transmitted through columns of gas at different distances. A strong LWIR light source will be used, such as a hot piece of metal or a human subject.

5. PROJECT PLAN

5.1 Budget Plan

Table 5.1 is the detailed budget for the entirety of the project. The components that will be present on the launch pad are highlighted in green.

Table 5.1 – Budget plan for NASA SL 2016

| ITEM | DESCRIPTION | QUANTITY | PRICE | LAUNCH PAD TOTAL | NON-LP TOTAL |
|---|-------------|----------|-------|------------------|--------------|
| | | | | | |
| Subscale & Full Scale Rocketry Parts | | | | | |

| | | | | | |
|---|-------------------------------|-----|----------|----------|----------|
| 7.5" Blue Tube | Airframe Body (fullscale) | 2 | \$139.95 | \$279.90 | |
| 7.5" Full Length Coupler | Coupler (fullscale) | 1 | \$91.95 | \$91.95 | |
| 7.5" Nose Cone | Nose Cone (fullscale) | 1 | \$87.95 | \$87.95 | |
| 5.5" Blue Tube | Airframe Body (subscale) | 2 | \$89.95 | | \$179.90 |
| 5.5" Full Length Coupler | Coupler (subscale) | 1 | \$55.95 | | \$55.95 |
| 5.5" Nose Cone - 21 in. | Nose Cone (subscale) | 1 | \$65.95 | | \$65.95 |
| Rail Buttons | Rail Buttons | 4 | \$1.25 | \$5.00 | |
| 18" Parachute | Parachute | 2 | \$53.00 | \$106.00 | |
| 48" Parachute | Parachute (subscale) | 1 | \$119.00 | | \$119.00 |
| Motor Mount Kit | Motor Mount (subscale) | 1 | \$7.50 | | \$7.50 |
| Motor Retainer | Motor Retainer (subscale) | 1 | \$26.75 | | \$26.75 |
| Motor Mount Kit | Motor Mount (fullscale) | 1 | \$9.95 | \$9.95 | |
| Motor Retainer | Motor Retainer (fullscale) | 1 | \$47.08 | \$47.08 | |
| 75mm Motor Casing | Motor Casing (full scale) | 1 | \$331.65 | \$331.65 | |
| 1/8" Quick Link | Quick Link | 2 | \$3.25 | | \$6.50 |
| Shear Pins | Sheer screws | 8 | \$2.95 | \$23.60 | |
| 5.5" Coupler Bulkhead | Coupler Bulkhead (sub scale) | 2 | \$7.25 | | \$14.50 |
| 7.5" Coupler Bulkhead | Coupler Bulkhead (full scale) | 2 | \$10.39 | \$20.78 | |
| Shock Cord | Shock Cord | 200 | \$0.92 | \$184.00 | |
| 9in Reusable wadding | Wadding | 4 | \$7.44 | \$29.76 | |
| StratoLogger | Altimeter | 4 | \$58.80 | \$235.20 | |
| Eye Bolts | Eye Bolts | 2 | \$4.50 | \$9.00 | |
| G10 Fiberglass | Fins | 10 | \$40.91 | \$409.10 | |
| 38 mm J400 6 grain | Subscale Motor | 2 | \$65.16 | | \$130.32 |
| 75mm L1115 4 grain | Fullscale Motor | 3 | \$246.95 | \$740.85 | |
| 1.5" PVC | 1.5" PVC 5' Length | 2 | \$4.68 | \$9.36 | |
| 1.5" PVC Cap | 1.5" PVC Cap | 4 | \$0.40 | \$1.60 | |
| | | | | | |
| Quadcopter Parts/Electronics | | | | | |
| Pixhawk | Controller | 1 | \$199.99 | \$199.99 | |
| 3DR uBlox GPS | GPS | 1 | \$90.00 | \$90.00 | |
| 3DR 900MHz Radio | Radio Set (Telemetry) | 1 | \$100.00 | \$100.00 | |

| | | | | | |
|--|---|---|----------|----------|----------|
| Spektrum DX7s + AR8000 Receiver | Radio (Control) + Controller | 1 | \$299.99 | \$299.99 | |
| Custom Electronics | Power regulation and parachute deployment | 1 | \$100.00 | \$100.00 | |
| External USB/LED | LED/USB port for Pixhawk | 1 | \$20.00 | \$20.00 | |
| Batteries | 6S LIPO | 2 | \$125.00 | \$250.00 | |
| Raspberry Pi | Processor | 1 | \$69.99 | \$69.99 | |
| Quadcopter Kit | Prototype Kit | 1 | \$122.87 | | \$122.87 |
| Drone Parachute | Parachute | 1 | \$70 | \$70 | |
| 1/4 in. x 4 ft. x 8 ft PureBond Birch Plywood | Plywood | 1 | \$24.92 | \$24.92 | |
| 1.75' Thick Green Delrin Acetal Plastic Sheet 3.25" X 3.875" Disc Ship | Delrin block | 1 | \$9.99 | \$9.99 | |
| 1x1x18" Carbon fiber square tubing | Arms | 2 | \$165.99 | \$331.98 | |
| KDE-CF155-DP Propeller Blades 15.5"X5.3, Dual Edition | Propeller blades | 4 | \$77.95 | \$311.80 | |
| KDE4014XF-380 Brushless Motor for Heavy Lift | Brushless motors | 4 | \$118.95 | \$475.80 | |
| Steel Ball Bearing | Ball bearing | 4 | \$3.28 | \$13.12 | |
| 1018 Carbon Steel Precision ACME Threaded Rod | | 2 | \$13.16 | \$26.32 | |
| Import 1ftx12inx1/4in thick acrylic plastic | Acrylic sheet | 2 | \$11.59 | \$23.18 | |
| Precision Ceramic-Coated Aluminum Shaft, 1/4" Diameter, 48" Length | Aluminum shaft | 2 | \$24.48 | \$48.96 | |
| 18-8 Stainless Steel Dowel Pin, 1/4" Diameter, 4" Length | Dowel pin | 4 | \$6.13 | \$24.52 | |
| 7.5" x .080 wall x 48" Airframe Blue Tube | Quadcopter Blue tube | 1 | \$80.96 | \$80.96 | |
| 7.5" x .080 wall x 16" Coupler Blue Tube | Quadcopter Body tube | 1 | \$28.75 | \$28.75 | |
| Plain Washer (inch) A and B X9 | Washers | 1 | \$6.64 | \$6.64 | |
| Hex Cap Screw X4 | Hex Cap Screw X4 | 1 | \$8.93 | \$8.93 | |
| Hex Nuts Inch series x4 | Hex Nuts Inch series x4 | 1 | \$6.22 | \$6.22 | |
| Washer A x8 | Washer A x8 | 1 | \$8.60 | \$8.60 | |
| Lock Washers x4 | Lock Washers x4 | 1 | \$7.50 | \$7.50 | |
| Hex Machine screw nut x4 | Hex Machine screw nut x4 | 1 | \$8.50 | \$8.50 | |

| | | | | | |
|--|--|---|---------|---------|------------|
| Cross Recessed Pan Head Machine Screw x4 | Cross Recessed Pan Head Machine Screw x4 | 1 | \$8.28 | \$8.28 | |
| Helical Spring Lock Washers x58 | Helical Spring Lock Washers x58 | 6 | \$4.57 | \$27.42 | |
| Hex Machine Screw Nut x53 | Hex Machine Screw Nut x53 | 1 | \$7.20 | \$7.20 | |
| Cross Recessed Pan Head Machine Screw x4 | Cross Recessed Pan Head Machine Screw x4 | 1 | \$11.00 | \$11.00 | |
| Hex Machine Screw Nut x16 | Hex Machine Screw Nut x16 | 1 | \$3.47 | \$3.47 | |
| hex machine screw nut x21 | hex machine screw nut x21 | 1 | \$3.15 | \$3.15 | |
| Planetary Gear Box | Planetary Gear Box | 1 | \$60.00 | \$60.00 | |
| | | | | | |
| | | | | | |
| Atmospheric Sensors | | | | | |
| Adafruit BME280 | Hum, Temp, Press | 1 | \$19.95 | \$19.95 | |
| Raspberry Pi Camera Module | Horizontal Pics | 1 | \$29.95 | \$29.95 | |
| 24x22mm Monocrystalline Solar Cell | Solar Panel | 1 | \$4.45 | \$4.45 | |
| Pi NoIR | IR Mapping | 1 | \$29.95 | \$29.95 | |
| IR Emitter | Abs. Spectro. | 2 | \$1.95 | | \$3.90 |
| IR Receiver Diode | Abs. Spectro. | 2 | \$9.95 | | \$19.90 |
| 9V Batteries | Power | 1 | \$15.23 | \$15.23 | |
| Raspberry Pi Battery | Power | 1 | \$49.95 | \$49.95 | |
| Raspberry Pi Battery Cables | Accessory to RP | 2 | \$1.95 | \$3.90 | |
| Serial Cable for Board | Accessory to RP | 1 | \$9.95 | | \$9.95 |
| Raspberry Pi B+ & 8GB SD Chip | Processing | 2 | \$49.95 | \$99.90 | |
| Arudino Due | Processing | 1 | \$49.95 | \$49.95 | |
| Data Logger | Data Storage | 1 | \$9.95 | \$9.95 | |
| 8 GB microSD card | Data Storage | 1 | \$6.56 | \$6.56 | |
| Breadboard | Processing | 1 | \$4.95 | | \$4.95 |
| 6xAA Battery Holder | Power | 1 | \$5.00 | \$5.00 | |
| AA batteries | Power | 1 | \$10.14 | \$10.14 | |
| | | | | | |
| | | | | | |
| Support | | | | | |
| Hotel (4 rooms for 5 nights) | | | | | \$2,600.00 |
| Gas (2 vans) | | | | | \$1,000.00 |

| | | | | | |
|----------------|--|--|-----------------------------|------------|-------------------------|
| Tolls (2 cars) | | | | | \$280.00 |
| | | | LAUNCH PAD TOTAL | | NON-LP TOTAL |
| | | | | \$5,724.79 | \$4,647.94 |

5.2 Funding Plan

AIAA at NU proposed to pursue project finances through internal funding via Northeastern Student Government Association (SGA), Northeastern grants, and external funding via corporate sponsorships.

Internal funding has increased since the Northeastern NASA SL 2016 Proposal submission. To start, AIAA at NU presented an itemized budget to the Northeastern SGA Finance Board and requested an equipment fund totaling \$2,698.30 for the fall semester. The request was successful and has since been approved, granting AIAA at NU financial support for prototyping equipment. In addition, AIAA at NU has submitted a grant request through the Northeastern Provost’s Undergraduate Research and Creative Endeavors Awards. This request was comprised of a detailed proposal of the ATMOS system, highlighting the uniqueness and originality of the design, proposed measurements, and the academic enrichment gained by students who are active in this endeavor. The recipients of this award will be announced by the end of November 2015. This funding would be used to purchase building materials for the full-scale design in the Spring 2016 semester.

In addition to internal funding, AIAA at NU has been working toward finalizing the framework required to reach out to potential corporate sponsors for the Fall 2015 and Spring 2016 semesters. The AIAA at NU Program Coordinator and the Funding Ambassadors have been working to establish a Northeastern approved list of companies in the aerospace industry to contact. As a result of the Summer I 2015 semester funding campaign, AIAA at NU is excited to confirm our first-ever corporate sponsor as Senior Aerospace Metal Bellows. The \$250 from the sponsorship will be used as partial support for both equipment and travel. AIAA at NU plans to finalize a new corporate outreach campaign by the end of the Fall 2015 semester.

5.3 Timeline

The timeline on the next page (Figure 5.3) is our projected schedule of events. Each color corresponds to a design group or documentation period. The blue diamonds represent projected launch dates and the red diamonds are NASA Student Launch milestones. Please refer to the key located above Figure 5.3.

- Payload Software
- Atmospheric Measurements
- Launch Vehicle
- General
- Controlled Descent
- Documentation
- NASA Deadline
- Launch Date

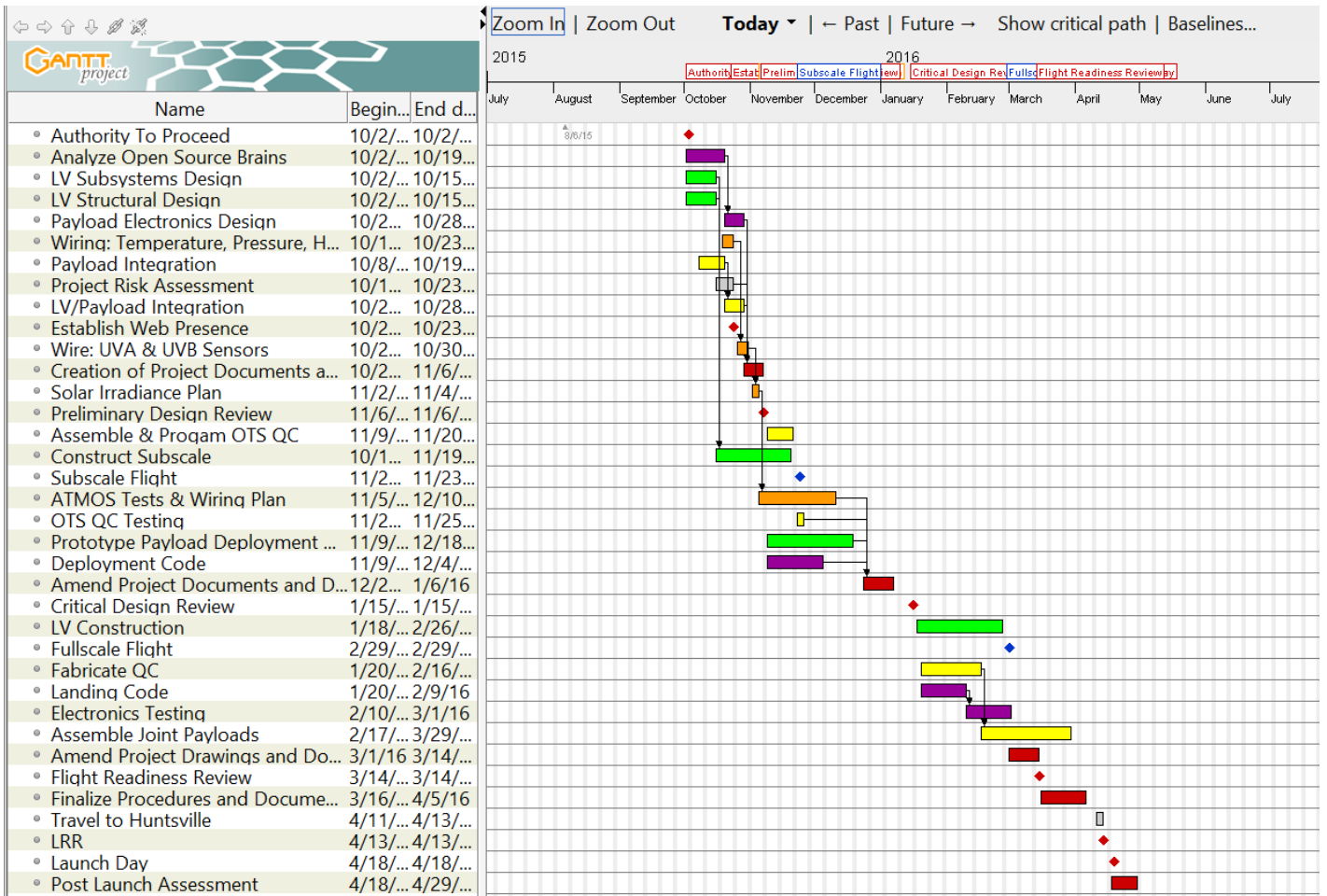


Figure 5.3 – Gantt chart for Northeastern AIAA NASA SL 2016

5.4 Educational Engagement

5.4.1 Goal of Education and Outreach

Throughout the course of the year, our team will conduct and assist with several educational outreach programs for middle schools and high schools in our community. Our goal for these programs is to convey the sense of excitement and wonder that we all felt when introduced to rocketry and space exploration for the first time. To accomplish this we will be continuing our partnership with Northeastern University’s Center for STEM Education and exploring new opportunities for outreach. Last year, we collaborated to reach more than 200 middle and high school students. This year, we hope to go beyond our previous year’s success and reach an even larger number of students.

5.4.2 Schedule of Coming Events

Table 5.4.2 – Schedule of future STEM events

| Event | Date | Expected Number of Students |
|--------------------|------------|-----------------------------|
| STEM Field Trip | 11/6/2015 | 50 |
| NEPTUN Class | 11/7/2015 | 10 |
| NEPTUN Class | 11/14/2015 | 10 |
| Fall 2015 Callback | 11/21/2015 | 30-40 |
| Engineering Month | February | 40-60 |

5.4.3 Description of Coming Events

STEM Field Trips

Northeastern's Center for STEM Education hosts field trips throughout the year for local K-12 schools. The schools select two out of the ten activities listed on the STEM website for their students to participate in during their visit to campus. When the schools choose to do the "Paper Rockets" activity, our organization assists by giving the students a lecture on rockets and rocket stability. This activity proves to be very popular with the visiting schools. After our presentation to the students, the students divide into pairs to begin construction. The paper nose cone is provided to the students, but they have the freedom to design the body and the fins however they would like. We help where necessary with the construction, typically helping the students to check how airtight their creations are. When construction is complete, the students measure the mass and length of their rockets and proceed outdoors to fly. AIAA volunteers time the launches so that students can use kinematic equations to calculate the altitude of their flight. To conclude, we discuss the results of the flights. Students identify what models worked best, and why. We have participated in one of these field trips this semester and plan to participate in two more in November and April. Some pictures from the field trip can be seen on the next page.



Figure 5.4.3.1 - Caroline Mueller E '19 assists two students with fin attachment for their paper rocket



Figure 5.4.3.2 - Students watch as two paper rockets compete for the highest altitude

NEPTUN Classes

We intend to teach two classes on SOLIDWORKS 3D through the Northeastern Program for Teaching by Undergraduates (NEPTUN). Members of our club will lead the class, and students will learn the basics of 3D modeling by making drawings and building small 3D parts. CAD is

a useful skill for all disciplines of engineering, and it's one we feel that students should get exposure to before they enter college.

Fall 2015 Callback

The Center for STEM Education holds a summer program every year for middle school students interested in STEM subjects. Students participate in activities that include problem solving, study, research, writing and communication skills, and cover subjects like biology, chemistry, physics, design concepts, and field excursions. In the fall, students who were involved in this program are invited back for the day in order to review, and learn more. Our organization will assist in that event with lectures and hands-on activities.

Engineering Month

The Center for STEM Education is planning an "Engineering Month," where Northeastern University student organizations visit local schools to provide demonstrations, small activities, and student panels. The details are currently being fleshed out, but the event will happen over the first three weeks of February.

5.4.4 Overall Status

In our proposal, we planned to have assisted with two STEM field trips, and educated 72 students. Due to rain, we were forced to cancel one of these field trips. Fortunately, the other field trip went well: we were able to teach 22 students about rocketry, and assist them in building their paper rockets. However, because we were unable to hold one of our events we are no longer on track to meet the 200 students. To compensate, we plan to reach out to local middle schools and high schools with offers to come to the schools to teach rocketry lessons and activities for their classes.

6. CONCLUSION

With our submission, we aim not only to complete the objectives set forward by the competition but also to design a controlled, reusable quadcopter descent module that can be used to take scientific readings at specific, controlled locations. The high precision of the CDLE allows us to land all scientific equipment in a predefined location with a high degree of accuracy and in a way that allows rapid data recovery and redeployment. Utilizing our unique recovery and deployment system from the launch vehicle, we will pioneer the task of taking a scientific payload in freefall and gaining complete control of its descent. During descent, the ATMOS payload will take atmospheric readings and photographs in different light spectrums. The combination of precision, autonomy, and scientific data taken ensures that our submission is unique and scientifically important.

Utilizing the two-charge separation system in the launch vehicle, we will be able to separate the quadcopter from the motor section and allow it to enter free fall on its own while the launch vehicle deploys its own recovery system. Seconds after the CDLE clears all the launch vehicle sections, it will begin its autonomous deployment sequence. The CDLE will unfold its arms, spin up all motors, and slow itself down until it is under controlled descent. Next, CDLE will use GPS location tracking

and constant communication with ground command in order to navigate to the landing area, coming in for a soft landing at the designated landing site. Once the CDLE has confirmed a successful landing, it will wirelessly relay all atmospheric data and images take back to ground command and then await recovery and redeployment.

Through a series of simulations and a real world test bed, we will be able to determine the validity and successes of our CDLE design. Through comprehensive preparation, we plan to ensure a high chance of success on launch day. These preparations and validations consist of running several trial landings on a test bed quadcopter, performing multiple subscale launches, and using GPS location to maintain constant awareness of the position of the quadcopter. In addition to these precautions, the CDLE has multiple fail safes that will trigger an emergency recovery method. The emergency recovery method, a backup parachute system, can be triggered by loss of communication, loss of telemetry, loss of control, or other errors. In the event the emergency recovery method is triggered, the CDLE can be safely recovered to allow determination of the cause of failure and to allow less repair before relaunch.

The ATMOS will take data during descent once per second on temperature, pressure, altitude, relative humidity, solar irradiance, and ultraviolet radiation. At various points throughout descent, the ATMOS will take pictures at various altitudes in the visible, near infrared, and long wave infrared spectrums. The sensors used on ATMOS will be tested in controlled conditions on the ground and compared against other sensors. The ATMOS itself will be tested in elevated conditions by bringing it to 100ft in a quadcopter, before the final test: a subscale rocket launch that will, at apogee, deploy the CDLE system, holding ATMOS.

The results of a successful trial of the deployment method could lead to further development and industry use. This controlled descent would be particularly useful in rapid controlled recovery of atmospheric data from high altitude collection systems, such as weather balloons. One example of this is the possibility of improving upon recovering equipment from collection systems that normally can take days to recover, such as a weather balloon, and allow for them to detach a data recovery system that can land itself in a preset location. This would permit for the possibility of quickly getting readings without having to rely on wireless transmission of data or worrying about losing equipment in the event of over or under inflation of a balloon. Tests such as these also validate the possibility of dropping quadcopters from high altitudes at the beginning of flight in order to allow for extended flight times without having to worry about using battery power to ascend to the desired height. The design could also be adapted to be utilized to carry payloads safely to the ground that would otherwise not be able to survive a hard landing, even with parachutes.

Looking towards the Student Launch 2016 competition, we hope to be able to display what the CDLE is capable of using the ATMOS and how these technologies can open up new possibilities for controlled descent missions and rapid data recovery.

APPENDIX A

| Milestone Review Flysheet | | | | | | | | | |
|---|-----------|----------------------------|-----------|-----------|---|-----------|--|-----------|-----------|
| Institution | | | | | Northeastern University AIAA | | | | |
| Milestone | | | | | PDR | | | | |
| Vehicle Properties | | | | | Motor Properties | | | | |
| Total Length (in) | | 127 | | | Motor Manufacturer | | Cesaroni | | |
| Diameter (in) | | 7.5 | | | Motor Designation | | L1115 | | |
| Gross Lift Off Weight (lb) | | 39.94 | | | Max/Average Thrust (lb) | | 385.48 / 251.78 | | |
| Airframe Material | | Blue Tube | | | Total Impulse (lbf-s) | | 5041.6 | | |
| Fin Material | | G10 fiberglass | | | Mass Before/After Burn | | 4.404 kg/ 2.01kg | | |
| Drag | | 302.5 N | | | Liftoff Thrust (lb) | | 385.48 | | |
| Stability Analysis | | | | | Ascent Analysis | | | | |
| Center of Pressure (in from nose) | | 87.608 | | | Maximum Velocity (ft/s) | | 633.2 | | |
| Center of Gravity (in from nose) | | 74.493 | | | Maximum Mach Number | | 0.57 | | |
| Static Stability Margin | | 1.75 | | | Maximum Acceleration (ft/s ²) | | 251.64 | | |
| Static Stability Margin (off launch rail) | | 1.75 | | | Target Apogee (From Simulations) | | 5366 | | |
| Thrust-to-Weight Ratio | | 6.18 | | | Stable Velocity (ft/s) | | 475.2 | | |
| Rail Size (in)/ Length (in) | | 1.5/120 | | | Distance to Stable Velocity (ft) | | 625 | | |
| Rail Exit Velocity (ft/s) | | 68.6 | | | | | | | |
| Recovery System Properties | | | | | Recovery System Properties | | | | |
| Drogue Parachute | | | | | Main Parachute | | | | |
| Manufacturer/Model | | Fruity Chutes | | | Manufacturer/Model | | Fruity Chutes | | |
| Size | | 18in for nose cone section | | | Size | | Two 18in and one 48in parachutes for booster section | | |
| Altitude at Deployment (ft) | | Apogee | | | Altitude at Deployment (ft) | | Apogee | | |
| Velocity at Deployment (ft/s) | | 0 | | | Velocity at Deployment (ft/s) | | 0 | | |
| Terminal Velocity (ft/s) | | 15.45 | | | Terminal Velocity (ft/s) | | 18.7 | | |
| Recovery Harness Material | | Kevlar Schock Cord | | | Recovery Harness Material | | Kevlar Shock Cord | | |
| Harness Size/Thickness (in) | | 0.23 | | | Harness Size/Thickness (in) | | 0.23 | | |
| Recovery Harness Length (ft) | | 15 | | | Recovery Harness Length (ft) | | 25 | | |
| Harness/Airframe Interfaces | | Eye bolts and bulk heads | | | Harness/Airframe Interfaces | | Eye bolts and bulk heads | | |
| Kinetic Energy of Each Section (Ft-lbs) | Section 1 | Section 2 | Section 3 | Section 4 | Kinetic Energy of Each | Section 1 | Section 2 | Section 3 | Section 4 |
| | 39.9 | 54.72 | | | | 39.9 | 54.72 | | |

| | | | | | | | | | |
|---------------------------------------|--|--|--|--|--|-----------------------|--|--|--|
| | | | | | Section (Ft-lbs) | | | | |
| Recovery Electronics | | | | | Recovery Electronics | | | | |
| Altimeter(s)/Timer(s) (Make/Model) | PerfectFlite Altimeters | | | | Rocket Locators (Make/Model) | BigRedBee GPS | | | |
| Redundancy Plan | In the bottom E-Bay there will be 2 batteries and in the top E-bay there will be two independent systems | | | | Transmitting Frequencies | ***Required by CDR*** | | | |
| Pad Stay Time (Launch Configuration) | 2 hours | | | | Black Powder Mass Drogue Chute (grams) | 3 | | | |
| | | | | | Black Powder Mass Main Chute (grams) | 3 | | | |

Milestone Review Flysheet

| | | | | | | | | | |
|--------------------|------------------------------|--|--|--|------------------|-----|--|--|--|
| Institution | Northeastern University AIAA | | | | Milestone | PDR | | | |
|--------------------|------------------------------|--|--|--|------------------|-----|--|--|--|

Autonomous Ground Support Equipment (MAV Teams Only)

| | | | | | | | | | |
|--------------------------------|---|--|--|--|--|--|--|--|--|
| Capture Mechanism | Overview | | | | | | | | |
| | | | | | | | | | |
| Container Mechanism | Overview | | | | | | | | |
| | | | | | | | | | |
| Launch Rail Mechanism | Overview | | | | | | | | |
| | ***Include Description of rail locking mechanism*** | | | | | | | | |
| Igniter Installation Mechanism | Overview | | | | | | | | |
| | | | | | | | | | |

Payload

| | | | | | | | | | |
|-----------|---|--|--|--|--|--|--|--|--|
| Payload 1 | Overview | | | | | | | | |
| | ATMOS (Atmospheric Topographic Measurements Optics Systems)-The Atmospheric measurements payload proposed by NASA. We will be measuring temperature, pressure, humidity, ultraviolet radiation, solar irradiance, atmospheric transmission, and plant density | | | | | | | | |

| | |
|-----------|---|
| Payload 2 | Overview |
| | CDLE (Controlled Descent Landing Experiment)-A custom quadcopter that will deploy from the rocket at apogee then make a controlled descent. The CDLE will contain the ATMOS payload to take measurements during descent |

Test Plans, Status, and Results

| | |
|-------------------------|---|
| Ejection Charge Tests | We plan to perform ejection test for both the sub-scale and the full-scale launch vehicles prior to first launch. We have not conducted any ejection tests at this date |
| Sub-scale Test Flights | The subscale launch is planned for November 21st, 2015 |
| Full-scale Test Flights | The full scale launch is planned for February 27th, 2016 |

Milestone Review Flysheet

| | | | |
|--------------------|------------------------------|------------------|-----|
| Institution | Northeastern University AIAA | Milestone | PDR |
|--------------------|------------------------------|------------------|-----|

Additional Comments

